Chapter 3: Mononuclear biscarbene complexes

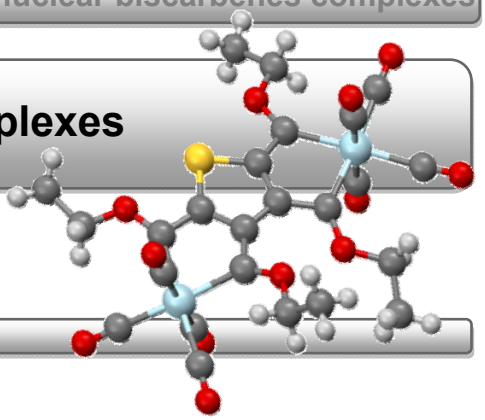

Synthesis and characterization

Introduction

Specific types of Fischer metal carbene complexes have found a niche in the broad spectrum of possibilities of this versatile species. A recent review by Sierra[1] described the distinct classes of Fischer carbene complexes segregated by their synthetic methodology. A small portion of this review was dedicated to the synthesis of carbene chelate complexes, characterized as such by Fischer [2] in 1981 and ironically, the first carbene complex ever synthesized by Chugaev [3] in 1925 was of this type (Figure 1.5, Chapter 1). Since then only a number of these classic Fischer carbene chelate complexes were synthesized with consideration to those containing N-heterocyclic moieties[4] thus further investigation was warranted. The methodology for synthesis of chelate metal carbene complexes was also limited. The use of lithiated species, free carbenes and isocyanide metal complex as starting materials proved to be the most dominant. As with other complexes synthesized and reported in this dissertation, the classic Fischer carbene methodology was applied to obtain these metal

[1] M.A. Sierra, *Chem. Rev*., **2000**, 100, 3591
[2] E.O. Fischer, W. Röll, U. Schubert, K. Ackermann, *Angew. Chem*., **1981**, *93*, 582,
[3] L. Chugaev, M. Skanavy-Grigorizeva, A. Posnjak, *Z. Anorg. Chem.,* **1925**, *148*, 37
[4] (a) E.O. Fischer, W. Röll. N.H.T. Huy, K. Ackermann, *Chem. Ber*., **1982**, *115*, 295
(b) U. Schubert, K. Ackermann, N.H.T. Huy, W. Röll, *J. Organomet.Chem*., **1982**, *232,* 155
(c) N.H.T. Huy, E.O. Fischer, J. Riede, U. Thewalt, K.H. Dötz, *J. Organomet. Chem.,* **1984,** *273***,** C29
(d) N.H.T. Huy, E.O. Fischer, H.G. Alt, K. H. Dötz, *J. Organomet. Chem.,* **1985,** *284***,** C9
(e) N.H.T. Huy, E.O. Fischer, *Nouv. J. Chim.,* **1985,** *9***,** 257
(f) N.H.T. Huy, P. Lefloch, J.M. Louis, M.J. Fetizon, *Organomet. Chem.,* **1986**, *311*, 79
(g) G. Rouschias, B.L. Shaw, *J. Chem. Soc. A,* **1971,** 2097
(h) A. Burke, A.L. Balch, J.H. Enemark, *J. Am. Chem.* Soc., **1970**, *92,* 2555
(i) J. Miller, A.L. Balch, J.H. Enemark, *J. Am. Chem. Soc*., **1971**, *93,* 4613
(j) W.E. Butler, J.H. Enemark, *Inorg. Chem.,* **1971**, *10*, 2416
(k) W.E. Butler, J.H. Enemark, *Inorg. Chem.,* **1973**, *12*, 540
(l) W.E. Butler, J.H. Enemark, *J. Organomet. Chem.,* **1973**, *49*, 233
(m) W.E. Butler, J.H. Enemark, J. Parks, A.L. Balch, *Inorg. Chem.,* **1973,** *12,* 451
(n) D.J. Doonan, A.L. Balch, *Inorg. Chem.,* **1974**, *13*, 921

carbene complexes. The obvious drawback was the tactical dilithiation on adjacent carbon atoms on an organic or organometallic moiety. Many compounds naturally contain two or more activated carbon atoms but few reside in flanking positions. Thiophene has two activated carbons but they reside on position two and five of the thienyl moiety. The degree of activation of the adjacent carbons, carbon 2 and 3, differ too much to allow for sequential lithiation. Modification of the thienyl moiety allowed for the synthesis of a metal chelate carbene complex by Crause[5]. The success of this synthesis laid in the elimination of the possibility that one of the activated protons react (Figure 3.1), but the limitation of this approach was obvious.

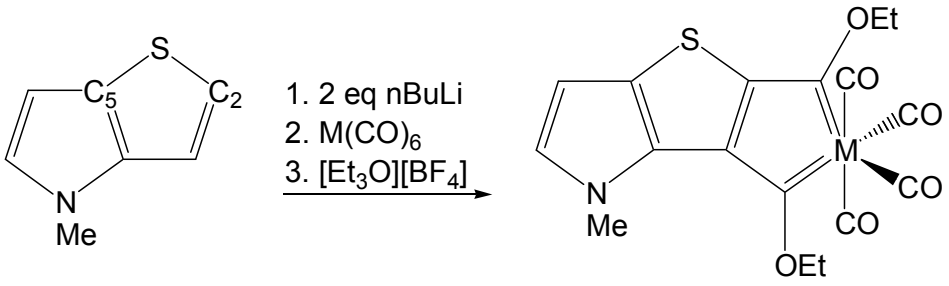

Figure 3.1: Mononuclear biscarbene synthesis on a modified thienyl derivative, M = Cr or W[5].

A more generally applicable method was required that could be used on a regular basis requiring minimal modification to accommodate a wide variety of starting materials. The obvious choice was to combine and modify existing methodology. As with the synthesis of the mononuclear metal biscarbene complex on benzene by Fischer[2], combination of organic synthetic methodology and classic Fischer metal carbene complex synthesis proved successful. By means of this inventive effort as a stepping-stone, slight modification may allow for a more widely applicable synthetic method. There were a few strategic proposals to resolve this type of problem and the most obvious was to reassess each reaction step independently and consider alternatives. From the success rate and common use[6] of the classic Fischer metal carbene complex synthesis, there was little improvement to be done, thus the only other tactic to reflect on was that of the starting material. The method

[5] C. Crause, PhD Thesis, *Synthesis and application of carbene complexes with heteroaromatic substituents,* **2004,** University of Pretoria.
[6] A. Hafner, L.S. Hegedus, G. de Weck, B. Hawkins and K.H. Dötz. *J. Am. Chem. Soc*., **1988,***110*, 8413

implemented by Fischer was the dilithiation of an aromatic starting material, but this method requires quite rigorous conditions. The dilithiation of phenylene was not obtainable from *o*-halopheneylene precursors or BuLi as they lead to the formation of polymers. The precursor was prepared by reacting the *o*-dibromobenzene with a Hg/Na amalgam to give phenylene mercury dimers or polymers, which on reaction with lithium metal affords the *o*-dilithium phenylene precursor used in Figure 3.2 below[7].

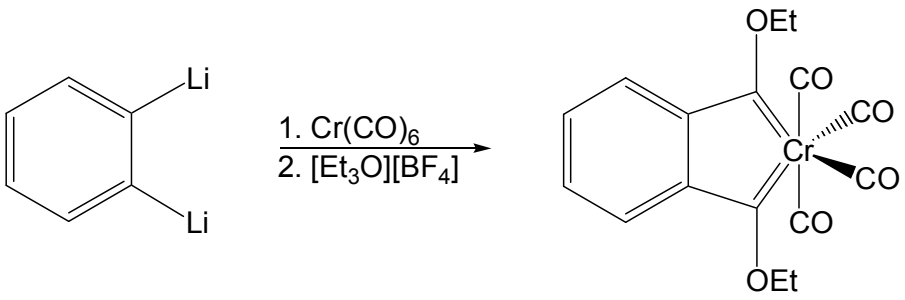

Figure 3.2: Chelate biscarbene synthesis from *o*-dilthiobenzene[4b].

To develop a general method for synthesizing classic Fischer chelate carbene complexes, comparable in ease to that of the classic Fischer monocarbene complex synthesis, a method for adjacent carbon atom activation had to be explored. Organic synthetic methods provided a range of possibilities, which was beyond the scope of this project, but what was of interest was halogenation of organic moieties, which activates carbon atoms[8]. The organolithium reagents were synthesized by a variety of different methods including lithium halogen exchange[9] as first described by Wittig[10] and additional methods consisted of reduction with metallic lithium[11], lithium base deprotonation[12] along with transmetalation[13]. Gilman exploited halogen-lithium

[7] G. Wittig, F. Bickelhaupt, *Angew. Chem.,* **1975**, *69*, 93
[8] L. Brandsma, H. Verkruijse, *Preparative polar organometallic chemistry I,* **1987,** Spinger-Verlag, Germany,
[9] (a) W.F. Bailey, J.J. Patricia, *J. Organomet. Chem.,* **1988**, *352*,1
(b) R.G. Jones, H. Gilman, In *Organic Reactions*, **1951**, *6,* R. Adams, Ed., Wiley, New York
[10] G. Wittig, U. Pockels, H. Dröge, *Chem. Ber.,* **1983***, 71*, 1903
[11] (a) C. Najera, J.M. Sansano, M. Yus, *Tetrahedron,* **2003**, *59*, 9255
(b) M. Yus, *Chem. Soc. Rev.,* **1996**, 155
[12] (a) E.J. Anctil, V. Snieckus, In *Metal-catalyzed cross-coupling reactions*, 2nd ed., **2004** , A. de Meijere, , F. Diederich, Eds., Wiley-VCH, Weinheim, Germany
(b) P. Beak, T.A. Johnson, D.D. Kim, S.H Lim, *Top. Organomet. Chem.,* **2003**, *5*, 139
[13] M. Pereyre, J-P. Quintard, A. Rahm, *Tin in Organic Synthesis*, **1986,** Butterworths, Stoneham

exchange to synthesize regiospecific compounds[14]. The incorporation of a halogen-lithium exchange in the synthesis of metal carbene complexes was not unprecedented and was applied in the synthesis of acyclic diamino free carbenes or ADCs, which can then be reacted with the appropriate transition metal to produce an ADC complex (Figure 3.3)[15].

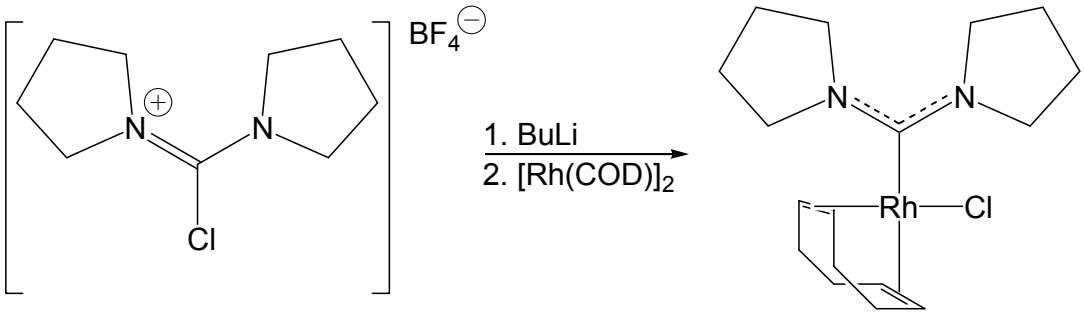

Figure 3.3: Synthesis of an ADC carbene complex utilizing lithium halogen exchange[15].

Lithium-halogen exchange was first investigated on arene[16] and has evolved considerably in range of application, but the basics remain the same.

$$LiR_1 + R_2X \longrightarrow LiX + R_1R_2$$

The interest in this field of organic chemistry was the ability of lithium to substitute a halogen under specific reaction conditions. The carbanion and the lithium carbon bond were considered a combination of covalent and ionic bonding and it was known that lithium halogen exchange was more favourable with alkenyl and aryl lithiums than with alkyl lithiums[17]. Lithium compounds are flammable in air, reactive towards oxygen containing compounds and react with water to give hydrocarbons. In addition, they show active towards quaternary ammonium halides[18]. Other metals such as sodium and potassium may have solubility difficulties and side

[14] H. Gilman, W. Langham, A.L. Jacoby, *J. Am. Chem. Soc.,* **1939,** *61*, 106
[15] D.R. Snead, I. Ghiviriga, K.A. Abboud, S. Hong, *Org. Lett*., **2009***, 11*, 3274
[16] J. Claydon, *Organolithiums: Selectivity for synthesis*, **2003,** *vol. 23 of Tetrahedron organic chemistry series,* Pergamon,
[17] D.E. Applequist, D.F. O Brien, *J. Am. Chem. Soc.,* **1963**, *85*, 743
[18] C.S. Marvel, F.D. Hacer, D.D. Coffman, *J. Am. Chem. Soc.,* **1927**, *49*, 2323

reactions as Wurtz coupling or ether cleavage. Many byproducts may be formed during these reactions. Formation of complex products are expected when more than one halogen is present. Reaction of *o*–dichlorobenzene and hexabromobenzene gave very complex insoluble products[18]. These reaction conditions similarly reflect that of metal carbene complex synthesis, the reaction is also accomplished at low temperatures in THF. For halogen substitution an extra equivalent of BuLi is added, one to react with the aromatic bromine and the second equivalent and the second to react with the BuBr. Bromination of organic moieties is a well-documented area with a wide breath of application. Considering only aromatic compounds, halogenation can easily be accomplished in a one-step reaction[19].

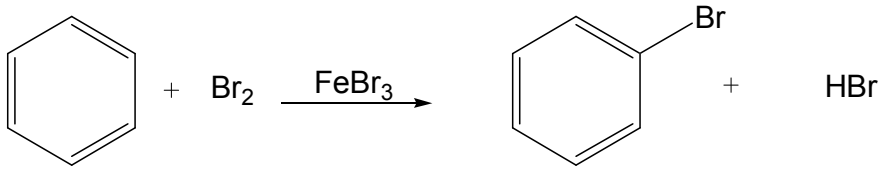

Figure 3.4: Monobromination of benzene[20].

Because brominated thiophene and other halogen derivatives are readily accessible[20]. The halogenated starting materials are available commercially and were purchased.

Synthesis

Using a brominated thienyl derivative as starting material creates the possibility for specific lithiation of selected carbons (Figure 3.5). The exchange reaction represents an equilibrium process[16] favouring the more stable or basic organolithium complex formation[21]. The reverse exchange reaction was slow to form the starting materials. The use of 2 equivalents of ^{t}BuLi makes the slow reversible reaction irreversible by eliminating the halide to form the iso-

[19] J. McMurry, *Organic chemistry, 5th ed.,* **2000**, Brooks/Cole, USA
[20] D.A. Guthrie, J.D. Tovar, *Org. Lett.,* **2008,** *10*, 4323
[21] H. Gilman, R.G. Jones, *J. Am. Chem. Soc.,* **1941,** *54*, 835

equivalents[22]. This eliminates the possibility of the alkyl halide byproduct interfering with subsequent reactions. This was not the case when using *n*BuLi. The reaction could be accelerated using ether solvents even at very low temperatures, which favours the halogen-metal exchange reaction above the formation of the ring triple bond when two neighbouring halogens are present in the molecule[23]. However, carbene complex synthesis in ether tends to be slow compared to THF. In contrast the lithiation of free thiophene was dependent on the acidity of the thienyl protons as discussed in Chapter 2, p60.

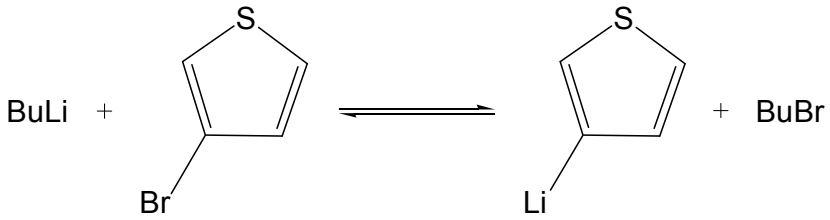

Figure 3.5: Lithium-halogen exchange for 3-bromothiophene.

The addition of the halogen on the 3 position allowed for selective lithium-halogen exchange on this position at -95˚C (Figure 3.5). This selectivity using halogen-lithium exchange reaction and application to different brominated thienyl starting materials allowed for the synthesis of the novel complexes, **B1** [Cr{2,3-C(OEt)C_4H_2SC(OEt)}$(CO)_4$], **B2** [Mo{2,3-C(OEt)C_4H_2SC(OEt)}$(CO)_4$], **B3** [W{2,3-C(OEt)C_4H_2SC(OEt)}$(CO)_4$], **B4** [η^5-(Cr{2,3-C(OEt)C_4H_2SC(OEt)}$(CO)_4$)$Cr(CO)_3$], **B5** [Cr{2,3-C(OEt)C_4H_2SC(NH_2)}$(CO)_4$], **B6** [2,3,4,5-C_4S{C(OEt)}$_4${$Cr(CO)_4$}$_2$] and **B7** [2,3,4,5-C_4S{C(OEt)}$_4C_4${$W(CO)_4$}$_2$]. Complex **B1** was synthesized using 3-bromothiophene and complex **B4** was synthesized using the same technique on [Cr{η^5-(3-bromothiophene)}$(CO)_3$]. Complex **B6** and **B7** were synthesized using 2,3,4,5-tetrabromothiophene as starting material. Complex **B1**, **B2** and **B3** were formed as byproducts from the reaction using 2,3,4,5-tetrabromothiophene and complex **B5** resulted from the aminolysis reaction of complex **B1**.

[22] (a) E.J. Corey, D.J. Beames, *J. Am. Chem. Soc.*, **1972**, *107,* 7210
(b) D. Seebach, H. Neuman, *Chem. Ber.,* **1974**, *1*, 7
[23] G. Köbrich, H. Trapp, *Chem. Ber.,* **1966**, *99,* 670

Synthesis of B1

Starting with the simplest starting material, a monobromothiophene, there are two possibilities, 2-bromothiophene and 3-bromothiophene. Using 2-bromothiophene was redundant as the 2 and 5 positions on thiophene was activated and was utilized without addition of bromine. In addition, the 3 and 4 positions of thiophene can not be used due to their low activation. With the bromine on the 3 position, both position 2 and 3 are exploited, position 2 because of the activation from the neighbouring sulphur atom and position 3 due to the presence of the bromine atom.

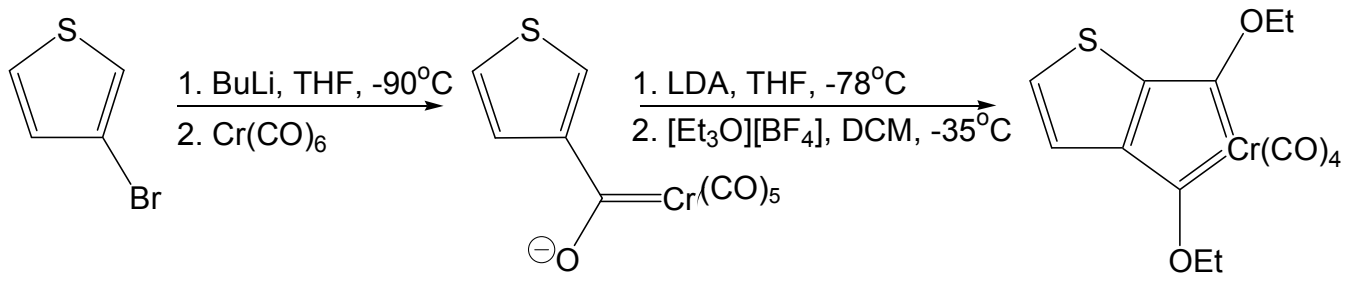

Figure 3.6: Synthesis and reaction conditions of B1.

Making use of both halogen-lithium exchange and activation of the thienyl protons, complex **B1** was synthesized (Figure 3.6). Addition of one equivalent BuLi at very low temperatures (-90ºC) only reacts with the bromine during which a colour change to yellow was observed. Addition of one equivalent LDA allowed for the removal of the second proton. This may be either at the 2 or 5 position but favouring the 5 position. To prevent the alternate reaction taking place at the 5 position, one equivalent hexacarbonyl chromium was added to form the intermediate metal acylate before the second equivalent of base was added. Closer inspection of the reaction mechanism (Figure 3.7) reveals that the nucleophillic carbon on the thienyl ring attacks an electrophillic carbonyl carbon atom. Thus, addition of a stoichiometric amount of metal hexacarbonyl material is vital. In the second attack, the carbon atom will attack the

carbonyl in the *cis* position of the first metal acylate, as the attack on a *trans* carbonyl is sterically unfavourable.

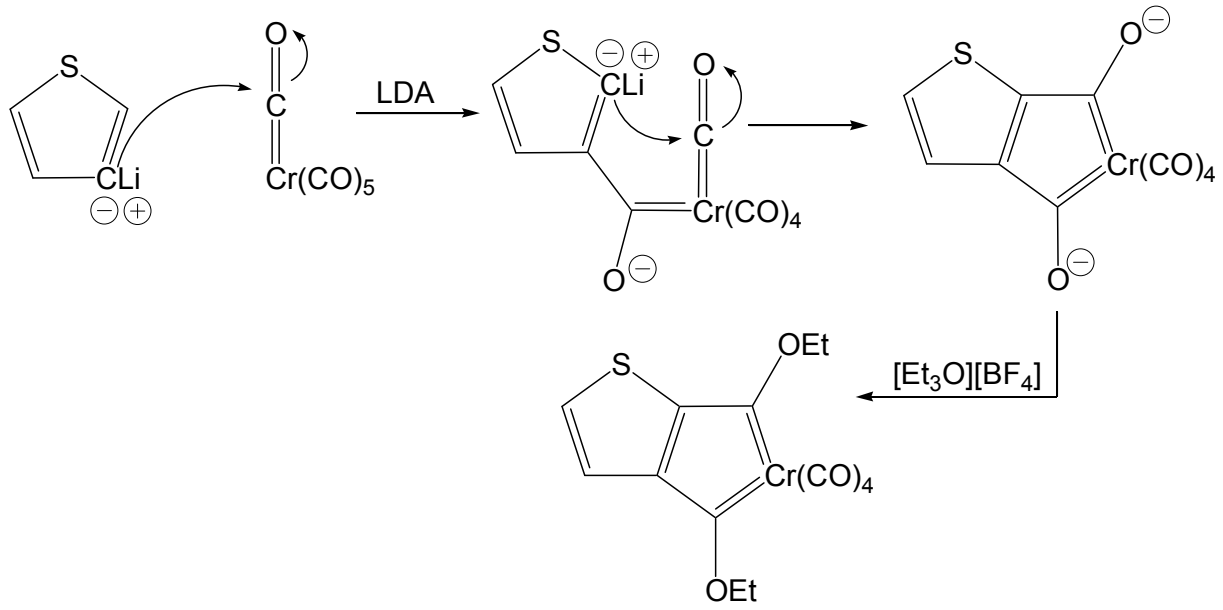

Figure 3.7: Reaction mechanism for the metal acylates of B1.

The metal acylate could further acidify the 2 proton, by withdrawal of electron density from the ring, resulting in a difference of acidities of the 2 and 5 proton positions. This allowed for the selective lithiation of the 2 position. The metal acylate acts as a protector of the electrophillic acyl carbon against further attack from strong bases[24] because of delocalization of the charge from the oxygen electron density to the metal. Addition of the hexacarbonyl metal results in a colour change to dark red. The proximity of the metal acylate on position 3 prevented the formation of a dinuclear biscarbene complex and facilitated the formation of a mononuclear biscarbene complex by additional stabilization of the chelate ring. The reaction was completed by alkylating both sites with triethyloxonium tetrafluoroborate in DCM at -35ºC to form a very dark coloured reaction mixture. From the reaction mixture of complex **B1**, three reaction products were observed, a minor yellow butylcarbene complex of chromium, a red

[24] S. Aiko, T. Fujimura, E. Nakamura, *J. Am. Chem. Soc.*, **1992**, *114*, 2985

monocarbene complex on the 3 position in high yield and the major constituent, the blue mononuclear biscarbene complex (**B1**) in a 40% yield.

Synthesis of B4

The same reaction synthesis and mechanism were applied to prepare complex **B4** (Figure 3.8). The starting material chromium η^5-(3-bromothiophene) tricarbonyl was synthesized in exactly the same way as described in Chapter 2, Figure 2.10, p61 using instead of thiophene, 3-bromothiophene. Again, the 3 position was the most reactive site because of the presence of the bromine atom and was easily removed with BuLi at cold temperatures after which the hexacarbonyl chromium was added to form the metal acylate.

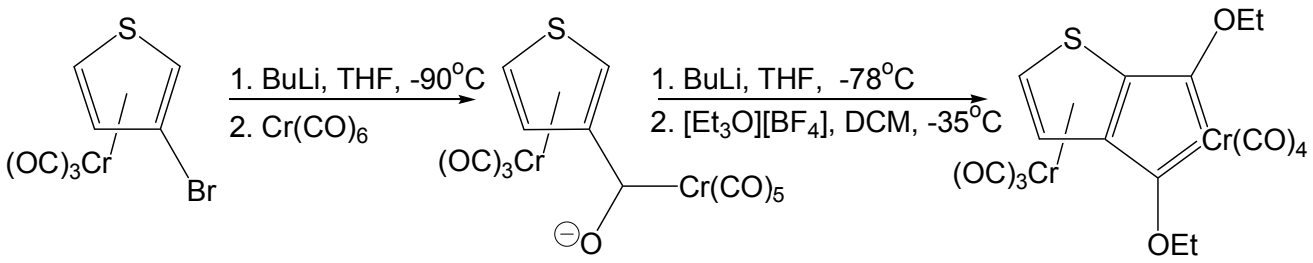

Figure 3.8: Synthesis and reaction conditions of B4.

The orange compound turn yellow after the first equivalent of base was added and turned red upon the addition of the hexacarbonyl chromium. The use of LDA for the second lithiation step was deemed unnecessary due to the additional activation of the ring protons owing to the electron withdrawal from the tricarbonyl metal fragment and was replaced with BuLi. The metal bisacylate was treated with alkylating agent at -35ºC in DCM to form the mononuclear biscarbene complex **B4**. From the reaction mixture the two major products could be successfully separated. The mononuclear biscarbene complex (**B4**) (20%), which was dark purple and a mixture of red monocarbene complexes were isolated. The monocarbene complexes could not be separated physically because of their similar composition but could be analyzed spectroscopically (NMR) and was determined to be the monocarbene complex on

position 2 and the monocarbene complex on position 3 of thiophene (Figure 3.9). Because the chromium tricarbonyl fragment was easily oxidizable, both π-coordinated and free thiophene monocarbene complexes were observed (I, II, III and IV, Figure 3.9) where as only complex I was observed as a byproduct from the synthesis of complex **B1**. The different quantities of the monocarbene complexes and the position of the carbene ligands from the reaction synthesis of complex **B1** and **B4** were explained by the activation of the starting materials. Less activation of the 2 position of 3-bromothiophene compared to chromium η^5-(3-bromothiophene) tricarbonyl was found. Thus lithiation of 3-bromothiophene favours the kinetic product, 3-lithiothiophene. In contrast the lithiation of chromium η^5-(3-bromothiophene) tricarbonyl favours the formation of the thermodynamic product chromium η^5-(2-lithiothiophene) tricarbonyl.

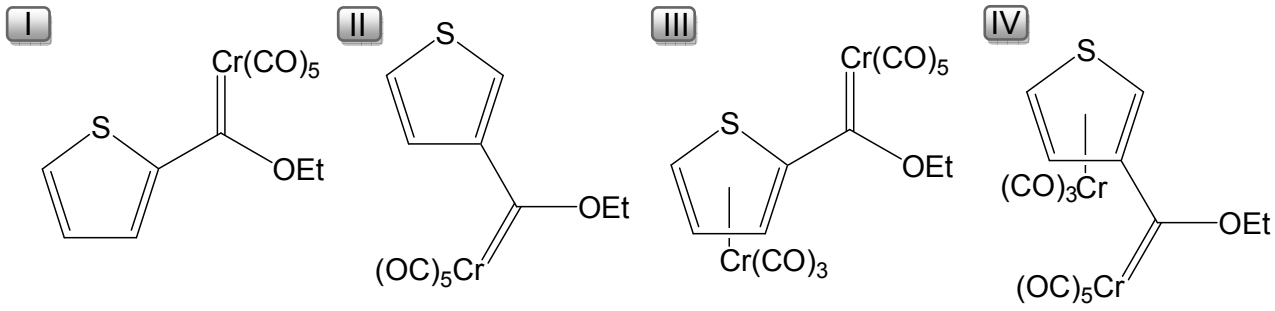

Figure 3.9: Reaction byproducts for the synthesis of B1 (I) and B4 (I-IV).

The lithium exchanged positions on chromium η^5-(3-lithiohiophene) tricarbonyl to form chromium η^5-(2-lithiothiophene) tricarbonyl, which is the thermodynamic more stable product. To favour the kinetic product the temperature must be kept very low during the first lithiation step, which is critical to the formation of the metal acylate in position 3 of complex **B4**. Difficulties with practically applying this was solubility of hexacarbonyl chromium at these temperatures. To increase solubility of hexacarbonyl chromium, the amount of reaction solvent THF was increased. Alternatively, the metal carbonyl was dissolved before addition and cooled to the desired temperature. The stability of complex **B4** was also much lower than complex **B1**.

Synthesis of B2, B3, B6 and B7

Changing the starting material to 2,3,4,5-tetrabromothiophene instead of 3-bromothiophene allowed for the synthesis of complexes, **B1** and **B2**. However, these complexes were obtained as byproducts for the target materials **B6** and **B7**. The same activation energy considerations applied to 2,3,4,5-bromothiophene as for free thiophene. The most activated positions were on the 2 and 5 carbon atoms, thus addition of BuLi resulted in the lithiation of these positions first (Figure 3.10).

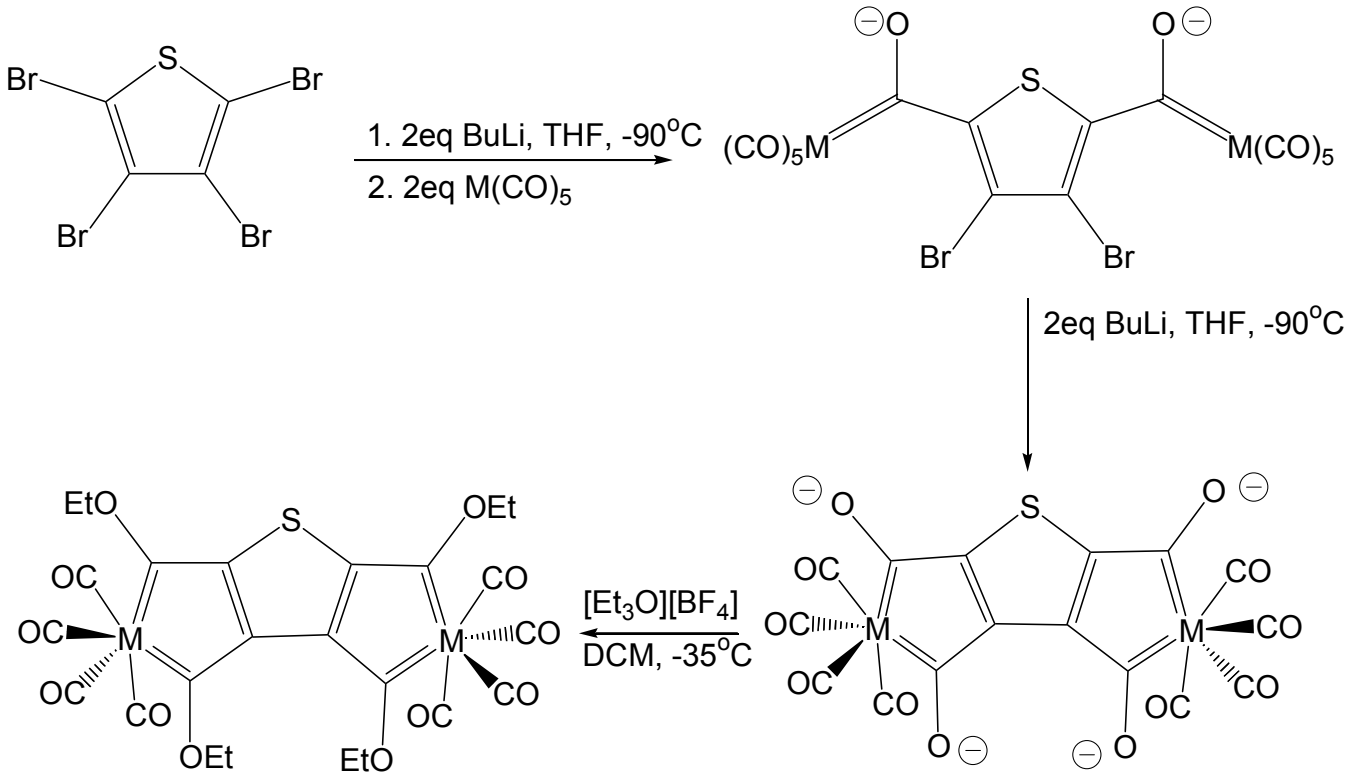

Figure 3.10: Synthesis and reaction conditions of B6 and B7.

Test reactions performed on 2,3,4,5-tetrabromothiophene to determine the influence and reactivity of the halogen substituent resulted in the determination of the reaction conditions

used during the synthesis of complexes, **B6-7**. Tetrabromothiophene was treated with one equivalent of BuLi at low temperatures. At temperatures below -95°C, no colour change was observed. At temperatures between -90°C and -95°C the colourless liquid turned light yellow. After the lithiation hexacarbonyl chromium was added to form the metal acylate and the mixture alkylated in DCM with triethyloxonium tetrafluoroborate. The reaction mixture was analyzed by ^{13}C-NMR spectroscopy to determine the presence of a monocarbene complex. From the reaction mixtures it was determined that a monocarbene complex was formed at the 2-position with bromines still present at the 3,4 and 5-positions. A second carbene complex on the 2-position showed that a bromine atom on the 5-position was exchanged with lithium and subsequently hydrolyzed to form the [Cr{C(OEt)3,4-C_4HBr_2}$(CO)_5$] complex. Commonly 2 equivalents of BuLi were added for each bromine to be exchanged. When this methodology was applied to lithiate and metalate all 4 positions of tetrabromothiophene a multitude of minor products were obtained which quickly decomposed on silica during separation. The reason for this is still unclear but it is suspected that, as with the lithiation of 1,2-dibromobenzene derivatives, polymerization occurs. The solution was to use only one equivalent of BuLi. During the lithiation of complex **B6** and **B7** the colourless liquid was observed to turn yellow and then murky orange as the temperature was allowed to increase from -90ºC to -78ºC. In contrast to free thiophene the 3 and 4 positions were also accessible due to the presence of the bromine atoms. After the addition of two equivalents of hexacarbonyl metal, the 3 and 4 positions were lithiated with 2 equivalents of BuLi. Upon the addition of the hexacarbonyl metal for the chromium, tungsten and molybdenum analogue the solution immediately turned darker. Again, because of the low temperatures at which these reactions were performed, the solubility of the hexacarbonyl metal was low, which was a problem. A considerable time was needed between the first and second lithiation step. The second lithiation procedure was done at -90ºC upon which the solution immediately turned pink and the colour intensified with time to become a very dark purple for each respective metal analogue. With the removal of the reaction solvent and resuspension in DCM the complex was alkylated with triethyloxonium tetrafluoroborate at -35ºC in DCM upon which the solution turned black. From the reaction mixture, three major products could be isolated with a large amount of a mixture of minor products were present. Due to low yields of these minor products, it was only possible to separate the major products. The three major products were a red monocarbene complex

mixture, a blue carbene monochelate complex (**B1**, **B2** and **B3**) and a purple to black carbene bischelate complex (**B6** and **B7**). The yields for each respective hexacarbonyl metal used were obtained from Chapter 4, Table 4.5, p169. For the reaction, using molybdenum hexacarbonyl, the yield and stability of the carbene bischelate complex was so low that the complex could not be positively identified and characterized. Complex **B6** and **B7** also have low stability compared to the carbene monochelate complexes **B1-3**. Upon decomposition the dark purple carbene bischelate complex turned dark green. This complex was suspected to be the thiophene-2,3,4,5-tetracarboxylic acid tetraethyl ester. The separation of the monocarbene complexes was difficult and the mixture was analyzed spectroscopically to determine the products that formed.

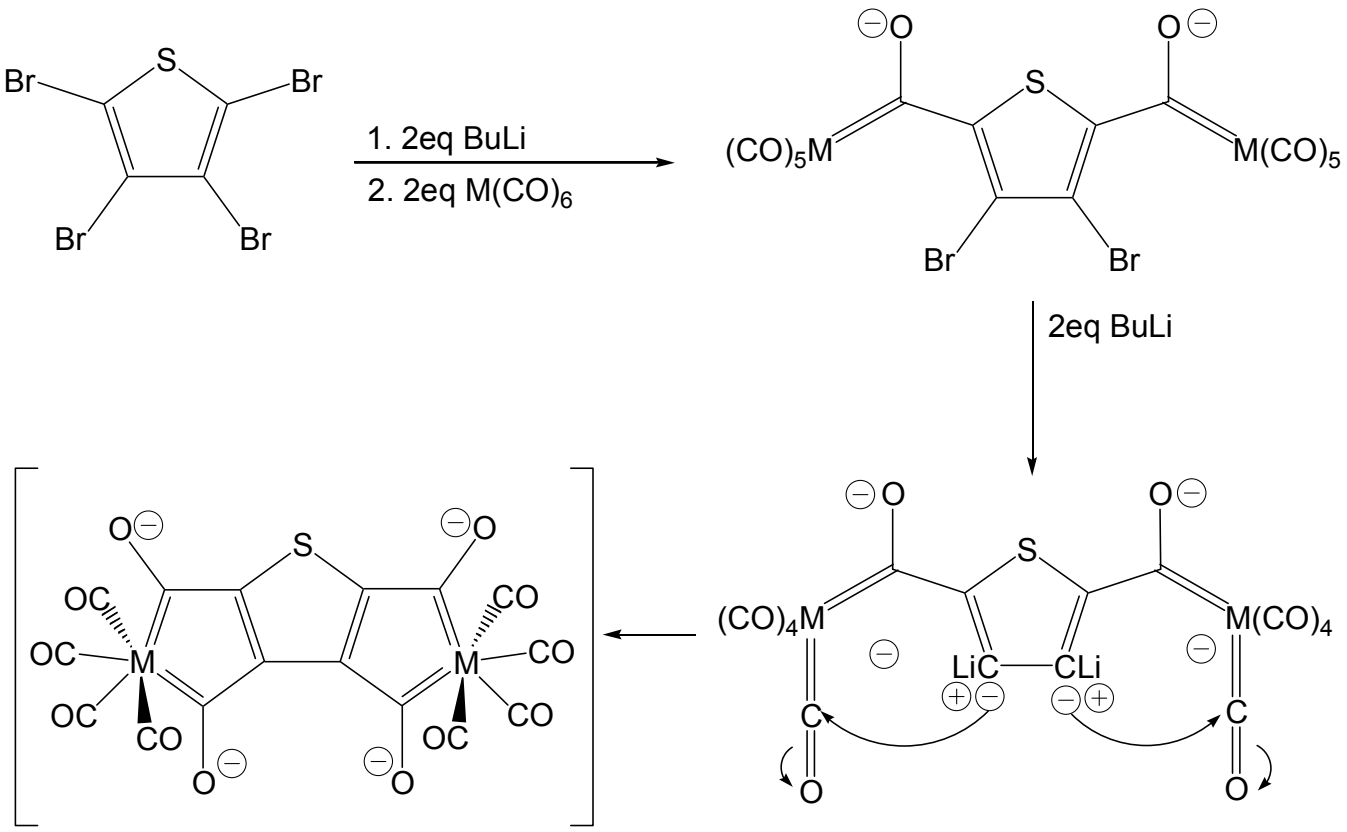

Figure 3.11: Reaction mechanism for the metal acylate formation of B6 and B7.

The formation of the carbene complexes were explained when looking at the reaction mechanism. The lithiation of the 2 and 5 position was sequential and the low temperatures at which the lithiation procedure was performed, can result in only one position being lithiated. In addition, considering that lithium-halogen exchange was an equilibrium reaction, the success of the metalation of both 2 and 5 position was limited as the equilibrium may shift after the first metal acylate was formed. The absence of chelate formation was also attributed to the lithium-halogen exchange and the limited amount of BuLi and hexacarbonyl metal added to the solution. The fact that there was carbene bischelate complexes formed during this reaction, but in a relatively small amount compared to the monocarbene and carbene monochelate complexes. This supported a lithium-halogen exchange equilibrium, even after the metal acylate was formed because some of the bromine atoms were not present when the complex was isolated. These bromine atoms were replaced with lithium atoms that were subsequently hydrolyzed.

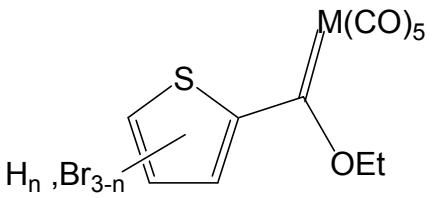

Figure 3.12: A byproduct formed during the reaction synthesis of B6 and B7.

Thus addition of excess hexacarbonyl metal or increasing its solubility and not adding excess BuLi, may result in higher yields of the carbene bischelate complex. In view of the monocarbene complexes formed during the reaction, the most obvious was the tribromothiophene monocarbene complex (Figure 3.12). The lithium-halogen exchange reaction allowed for several other monocarbene products to form and the subsequent hydrolysis of the lithium atom to form the final monocarbene complex. Because the lithiation of the 2 and 5 position was favoured and the hexacarbonyl metal was added before the second lithiation step the formation of the metal acylate on position 3 or 4 was not plausible. Thus the only possible carbene complexes were on the 2 or 5 position of thiophene ring. The difference in carbene complexes was the position and number of halogen atoms present and the

following complexes are possible of which six was identified; [Cr{2-C(OEt)(3,4,5-C_4Br_3S)}$(CO)_5$], [Cr{2-C(OEt)(4,5-C_4Br_2HS)}$(CO)_5$], [Cr{2-C(OEt)(3,5-C_4Br_2HS)}$(CO)_5$], [Cr{2-C(OEt)(3,4-C_4Br_2HS)}$(CO)_5$], [Cr{2-C(OEt)(5-C_4BrH_2S)}$(CO)_5$], [Cr{2-C(OEt)(4-C_4BrH_2S)}$(CO)_5$], [Cr{2-C(OEt)(3-C_4BrH_2S)}$(CO)_5$] and [Cr{2-C(OEt)(C_4H_3S)}$(CO)_5$].

Synthesis of B5

To determine the reactivity of the carbene monochelate complex towards a primary amine, complex **B1** was aminolyzed. Aminolysis was done in ether while gaseous ammonia was bubbled through the solution. The blue colour of complex **B1** changed slightly as well as the polarity of the products, as observed by following the reaction using thin layer chromatography. Generally aminolysis of a carbene complex is very favourable and the ethoxy groups are readily exchanged. During this reaction, only a single ethoxy group was exchanged and the conversion was almost 100% (Figure 3.13). A singular exchange of this kind has not yet been reported before, for any other multicarbene complexes and opens unique opportunities in organic chemistry.

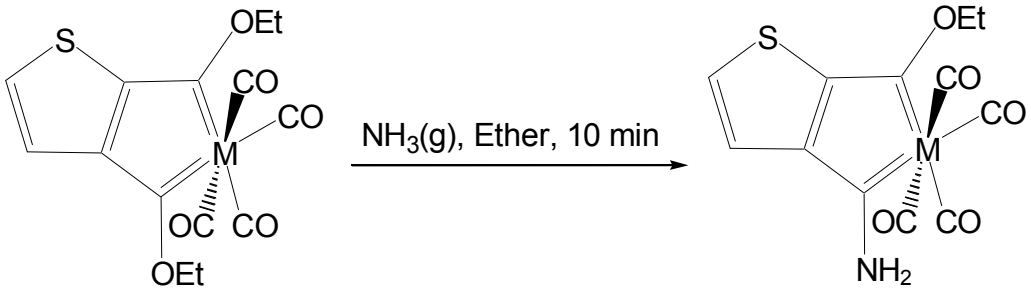

Figure 3.13: Aminolysis of B1, M = Cr.

Reacting the chelate carbene complex (**B1**) for a prolonged period to obtain the diaminochelate carbene complex resulted in the decomposition of the carbene chelate complex. This ascribed to an increase in the bonding character of the amine to the carbene carbon and a consequent decrease in the bonding of the carbene to the metal of both carbene

carbons. The strained and weaker geometry of the conjugate ring contributes to the ring opening and complex decomposition. Aminolysis of carbene complexes often lead to more stable complexes but the exchange of only a single ethoxy group with an amine suggested the stability of the ethoxy group on the carbene carbon closest to the sulphur atom was higher, resulting in only the ethoxy group of lower stability being exchanged (Figure 3.14). The higher stability of one carbene is a consequence of stabilization by electron delocalization from the thienyl ring.

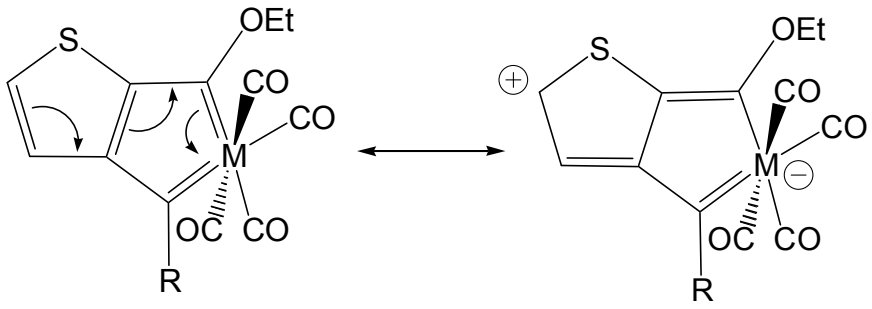

Figure 3.14: Movement of electron density in the π-conjugated ring system. R=OEt, NH_2.

Characterization

Characterization of the carbene chelate complexes was done by ^{1}H and ^{13}C-NMR (**B1-7** and byproducts), IR (**B1-3** and **B5-7**) and UV spectroscopy (**B1, B2, B6** and **B7**), mass spectrometry (**B7**) and X-Ray diffraction (**B1-3, B5** and **B7)**.

^{1}H-NMR spectroscopy

Elucidation of B1-4

The resonance of the thienyl proton neighbouring a carbene ligand is affected most and was shifted furthest downfield as observed for the chromium biscarbene complex $[(CO)_5Cr\{C(OEt)C_4H_2SC(OEt)\}Cr(CO)_5]$ where the ring protons were found at 8.06 ppm

($CDCl_3$)[25] for H3 and H4. This was also true for the monocarbene complex with the carbene ligand in the 2 position, such as [Cr{C(OEt)C_4H_3S}$(CO)_5$] where the proton resonance were found at (H3) 8.14, (H4) 7.20 and (H5) 7.80 ppm[26] respectively compared to the peaks at (H2 and 5) 7.20 and (H3 and 4) 6.96 ppm[27] for thiophene.

Table 3.1: ^{1}H-NMR data of B1 -4.

Assignments	Complexes							
	Chemical shift (δ) and coupling constant (*J*, Hz)							
	B1 (C_6D_6)				B2 ($CDCl_3$)		B3 (C_6D_6)	
Proton	δ		*J*				δ	*J*
	(C_6D_6)	($CDCl_3$)	(C_6D_6)	($CDCl_3$)				
H4	6.60	8.83 (d)	5.1	5.0	7.60 (d)	5.1	7.31 (d)	5.1
H5	6.43	7.55 (d)	5.1	5.0	6.92 (d)	5.1	6.96 (d)	5.3
O**CH_2**CH_3	4.47 (p)	4.77 (q)	7.1	6.8	4.76 (q)	7.1	4.45 (q)	7.1
		4.73 (q)		6.8	4.75 (q)	7.1	4.44 (q)	7.1
OCH_2**CH_3**	1.12 (t)	1.63 (t)	7.1	7.3	1.61 (t)	7.1	1.86 (t)	7.1
	1.09 (t)	1.64 (m)		7.3	1.60 (t)	7.1	1.86 (t)	7.1

The situation may differ for **B1**-**4** because the biscarbene 5-memebered chelate ring was condensed to the thiophene ring at position 2 and 3 and as a result affected the π-conjugation in the complex. The protons were deshielded by the carbene ligand such that they were shifted upfield. The movement of charge in the carbene monochelate complex of **B1-4**, generates a positive charge on the 5 position of the thienyl carbon (Figure 3.14). The electron density was shared with the metal chelate carbene complex, deshielding the thienyl protons and the resonance observed for the H4 proton was more downfield than the H5 chemical shift values in all cases, **B1-4** (Figure 3.16).

[25] Y.M. Terblans, S. Lotz, *J. Chem. Soc., Dalton Trans.*, **1997**, 2177
[26] S. Gronowitz, *Adv. Heterocycl. Chem.*, **1963**, *1*, 1
[27] R.J. Abraham, J. Fischer, P. Loftus, *Introduction to NMR Spectroscopy,* **1988,** John Wiley and Sons

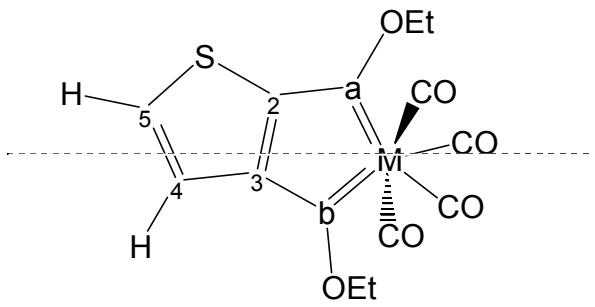

Figure 3.15: Representation of the different environments of B1-3.

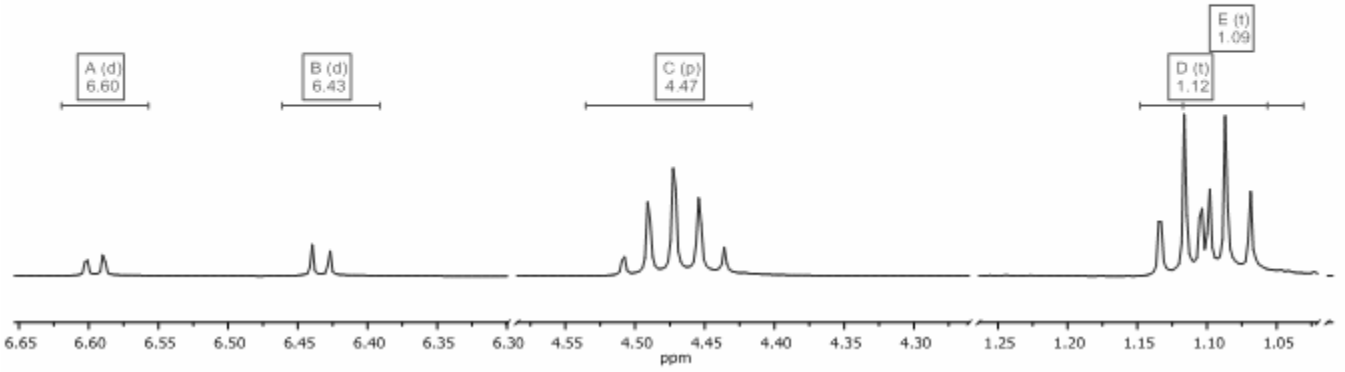

Figure 3.16: ^{1}H-NMR spectrum of B1 in deuterated benzene.

Two quartets (overlapping) that appears to be a pentet and two triplet resonances were observed for complex **B1** ($CDCl_3$), **B2** and **B3** (C_6D_6). The magnitude of the combination of electron density to the electrophillic carbene carbon atom from the ethoxy substituents differ to the extent that the metal (same) and thiophene (differ) can stabilize the charge. Consequently the oxygen attached to the carbene **a** will be less involved in stabilizing the carbene carbon and an ethoxy resonance is expected upfield from the other ethyl of second ethoxy group on the carbene carbon **b**, for which no favourable π-delocalization exists from the thiophene ring (Figure 3.14). The difference in chemical environments was also distinguished in the separation of the methylene protons (Figure 3.17). The ethoxy group on carbene **a** is close to

the thiophene sulphur whereas the ethoxy group on carbene **b** is not. This causes two separate triplet and quartet signals to be observed for the ethoxy groups on the two identical carbene ligands.

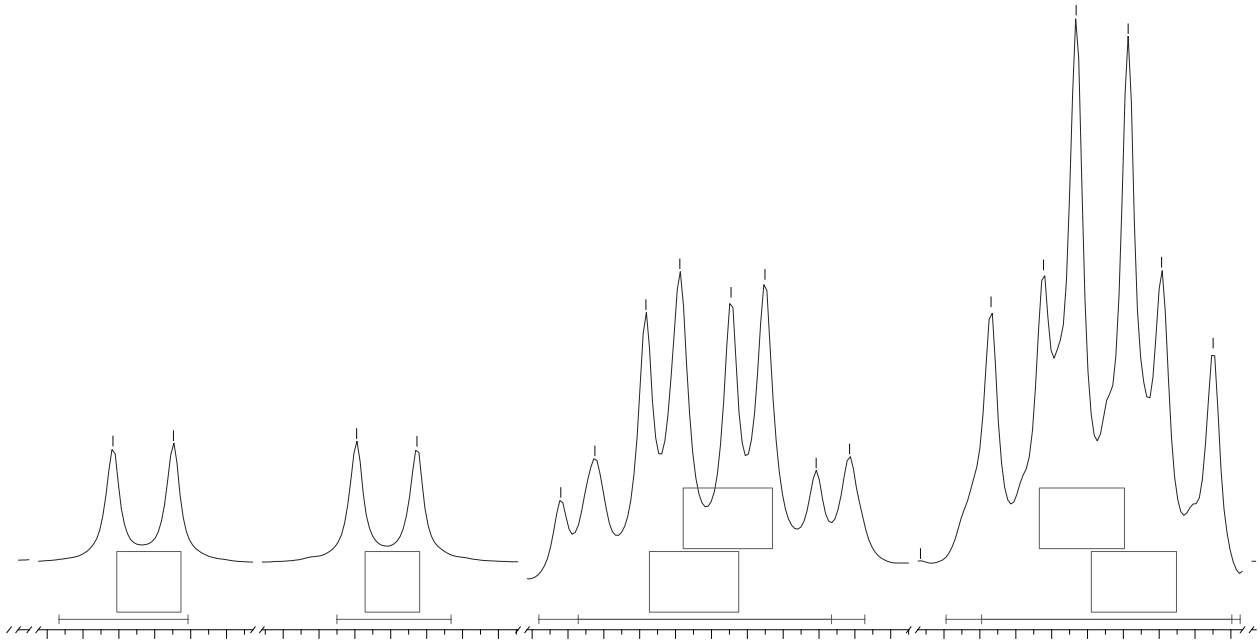

Figure 3.17: ^{1}H-NMR spectrum of B2 in $CDCl_3$.

This duplication of ethoxy proton resonances was not observed for the carbene chelate complexes, $[M(C\{(OEt)N(Ph)\})_2(CO)_4]$ where M = Cr, and W. These complexes are symmetrical, the resonance of the CH_2 protons were reported as single quartets at ($CDCl_3$) 4.7 (Cr) and 4.8 ppm (W) respectively[28]. In addition, the CH_3 resonances were reported as single triplets at 1.3 (Cr) and 1.4 (W) ppm. These values correspond to those obtained for complex **B1-4** (Table 3.1).

[28] N.H.T. Huy, C. Pascard, E.T.H. Dau, K.H. Dötz, *Organometallics,* **1988,** *7,* 590

Elucidation of B5

Table 3.2: ^{1}H-NMR spectral data of B5.

Assignments	Complexes
	Chemical shift (δ)
	B5 ($CDCl_3$)
Proton	δ
H4	7.78 (br)
H5	6.81 (br)
$OC\mathbf{H_2}CH_3$	4.94 (br)
$OCH_2\mathbf{CH_3}$	1.76 (br)
$N\mathbf{H_2}$	9.52 (br)

The contribution of the carbene substituents was seen from the spectrum of **B5** (Table 3.2). The ethoxy CH_2 chemical shift of **B5**, 4.94 ppm, was downfield compared to the same protons in complex **B1** where the chemical shifts of the ethoxy groups on carbene carbon **a** and **b** were recorded at 4.77 and 4.73 ppm, respectively. This downfield shift corresponded to the ethoxy CH_2 protons of complex **B5** being more deshielded for which there is no clear explanation. Because of the NH_2 present, the proton spectrum chemical shifts were broad and HETCOR experiments were used to assign the ^{1}H-NMR spectrum.

Elucidation of B4

Table 3.3: ^{1}H-NMR data of B4.

Assignments	Complexes
	Chemical shift (δ)
	B4 (C_6D_6)
Proton	δ
H4	6.02 (m)
H5	6.02 (m)
O**CH_2**CH_3	4.40 (m)
OCH_2**CH_3**	1.36 (m)
	1.45 (m)

Complex **B4** has an additional coordinated chromium tricarbonyl fragment on the thienyl moiety. The chromium tricarbonyl fragment is bound to the π-electron cloud[29] and causes the characteristic upfield shift of the thienyl protons. The thienyl proton resonances of complex **B4** are shifted upfield byan average value of 0.6 ppm compared to the non-coordinated mononuclear chelate carbene complexes **B1-3**. The pull of electron density in opposing direction from the biscarbene metal fragment and the coordinated chromium tricarbonyl fragment results in the thienyl ring to become electron deficient. This contributed to the localization of the double bonds ensuing in the decrease of the aromaticity of the heteroarene ring. Combined with the downfield shift that was characteristic for a carbene metal fragment, the proton resonances of the thienyl protons H4 and H5 of **B4** were seen as a broad peak at 6.02 ppm (Table 3.1). The ethoxy CH_2 protons were shifted slightly upfield, at 4.40 ppm when compared to complex **B1** where they were recorded at 4.47 ppm. The electron draining

[29] A. Mangini, F. Taddei, *Inorg. Chim. Acta.,* **1968**, *2,* 12

tricarbonyl fragment influences the thienyl rings ability to stabilize the electrophillic carbene carbon.

Elucidation of byproducts formed for the reaction synthesis of B4

The preparation of complex **B4** also displayed the formation of several monocarbene complexes. The monocarbene byproducts formed during the reaction were characterized with NMR and the data is summarized in Table 3.4. Four possible products were expected (Figure 3.18), complex I and III were the thermodynamically favoured products due to exchange of the bromine and complex II and IV were the kinetically favoured products. The difference in chemical shift of the ring proton on free thiophene and coordinated thiophene allowed for the demarcation between the different monocarbene complexes. From the spectrum, only three of the four possibilities were observed. Complex I, III and IV were identified. The identification of complex IV verified that complex II was present but that the chromium tricarbonyl fragment was removed.

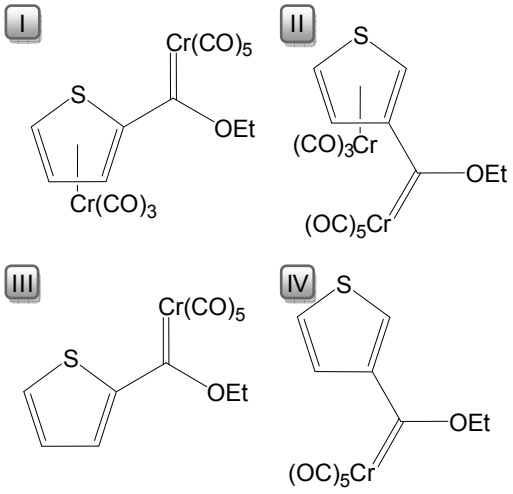

Figure 3.18: The byproducts of the synthesis of the π-coordinated chelate chromium biscarbene complex

Complex I has been previously synthesized and characterized by Terblans[25] and III was reported by Gronowitz[26] but complex II and IV have not previously been reported. These complexes were identified as byproducts from the synthesis of complex **B4**.

Table 3.4: The NMR data of the monocarbene byproducts of the synthesis of B4.

Assignments	Complexes					
	Chemical shift (δ) and coupling constant (*J*, Hz)					
	I		III		IV	
Proton	δ	*J*	δ	*J*	δ	*J*
H2					7.45 (s)	
H3	6.73 (d)	3.4	8.24 (d)	4.0		
H4	6.01 (dd)	3.6, 3.6	7.21 (m)		7.68 (d)	5.0
H5	5.93 (d)	3.7	7.68 (d)	5.0	8.24 (d)	5.0
O**CH$_2$**CH$_3$	5.06 (q)	7.0	5.16 (q)	7.0	5.00 (q)	7.0
	5.04 (q)					
	4.98 (q)					
	4.96 (q)					
OCH$_2$**CH$_3$**	1.54 (t)	7.0	1.65 (m)		1.66 (t)	7.0

Because of the difference in carbene ligand position of the two monocarbene complex analogues (III and IV) on the 2 and 3 position it was easy to distinguish between the separate complexes (Table 3.4). Likewise, the difference in position of the carbene ligand of complex I and II should be easily distinguishable but only complex I was identified. Complex I shows proton resonances corresponding to reported values[25] of the monocarbene analogue at δ 6.73, 6.01 and 5.93 for the H3, H4 and H5 protons in that order. Deshielding of these protons the chromium tricarbonyl fragment results in an upfield shift. The thienyl ring pattern for complex III shows the same proton resonance pattern as complex IV only shifted downfield, two doublets at δ 8.24 (H5) and δ 7.68 (H4) and a singlet at δ 7.45 (H2) for IV, and for III, a doublet at δ 8.24 (H2), a multiplet at δ 7.21 (H3) and a doublet at δ 7.68 (H5). With the carbene ligand on the 3 position of thiophene, the chemical shift of the H2 proton of complex IV (δ 7.45) was

upfield from the H3 resonance of III (δ 7.68) because of the influence of both the sulphur and the carbene metal ligand. The carbene ligand influence on the H4 and H5 protons was more due to the proximity of the carbene ligand and results in the downfield shift of these signals.

Elucidation of B6 and B7

The proton resonances of **B6** and **B7** showed only the chemical shifts being those from the carbene ethoxy groups (Table 3.5). Again the signals were slightly shifted apart due to the influence of the sulphur atom being two bonds or four bonds away from the two carbene carbons. Instead of four chemical shifts for each CH_2 group there were only two because of the symmetry in the molecule (Figure 3.19).

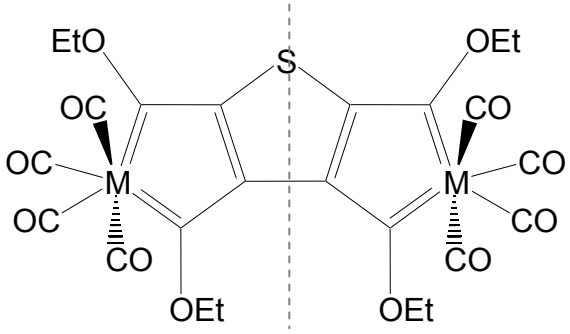

Figure 3.19: Plane of symmetry for B6 and B7.

Two separate monocarbene ligands on the 2 and 5 position of thiophene have the ethoxy CH_2 and CH_3 proton resonances recorded in $CDCl_3$ at δ 5.21 and δ 1.69 for the chromium analogue and δ 4.98 and δ 1.68 for tungsten[30]. The influence of four carbene ligands attached to the thienyl ring in **B6** and **B7** is to distribute charge more equally through the ring system (Figure 3.19) and results in less prominent contributions from the ethoxy substituents. This manifested in the ethoxy proton resonances which were found less downfield relevant to the 2,5-thiophene biscarbene complexes.

Table 3.5: ^{1}H-NMR data of B6 and B7.

Assignments	Complexes							
	Chemical shift (δ) and coupling constant (*J*, Hz)							
	B6				B7			
Proton	δ		*J*		δ		*J*	
	($CDCl_3$)	**(C_6D_6)**	**($CDCl_3$)**	**(C_6D_6)**	**(C_6D_6)**	**($CDCl_3$)**	**(C_6D_6)**	**($CDCl_3$)**
$OC\mathbf{H_2}CH_3$	4.76 (q)	4.47 (q)	7.1	7.0	4.45 (q)	4.27 (m)	7.2	
	4.84 (q)	4.39 (q)	6.9	6.8	4.45 (q)		7.3	
$OCH_2\mathbf{CH_3}$	1.44 (t)	1.07 (t)	6.9	6.9	1.86 (t)	1.12 (t)	7.1	7.2
	1.43 (t)		6.9		1.86 (t)		7.1	

The resonances of the methylene protons were observed to have a ± 0.3 ppm shift when considering the two reference solvents used. These protons were moved downfield and the ability of the larger tungsten metal to backdonate to the carbene carbon leads to a more shielded ethoxy substituent. From Figure 3.20 the difference in the ability of the condensed ring arrangement to transfer charge across the system, seen to be symmetrical in contrast to that of the carbene monochelate in Figure 3.14, p109. The chemical shift observed for the CH_2 protons were only due to the different environments. Upon decomposition, the dark purple chromium bischelate carbene complex turned dark green. The NMR spectrum of this complex showed two overlapping quartets at (C_6D_6) 4.54 ppm (*J* = 7.3 Hz) and a bordering quartet, 4.25 ppm (*J* = 7.0 Hz). From the integration values of the two regions, they represented four methylene protons for the first set and second set of quartets. There was no duplication of the second set of quartets thus the two protons were in similar environments. These values indicated the oxidation of a carbene moiety to an ester. The carbene metal substituent methylene protons were recorded at ($CDCl_3$) 5.20 ppm and 4.37 ppm for the ester CH_2 protons[30].

[30] Y.M. Terblans, *Thiophene bimetallic carbene complexes*, **1996**, University of Pretoria

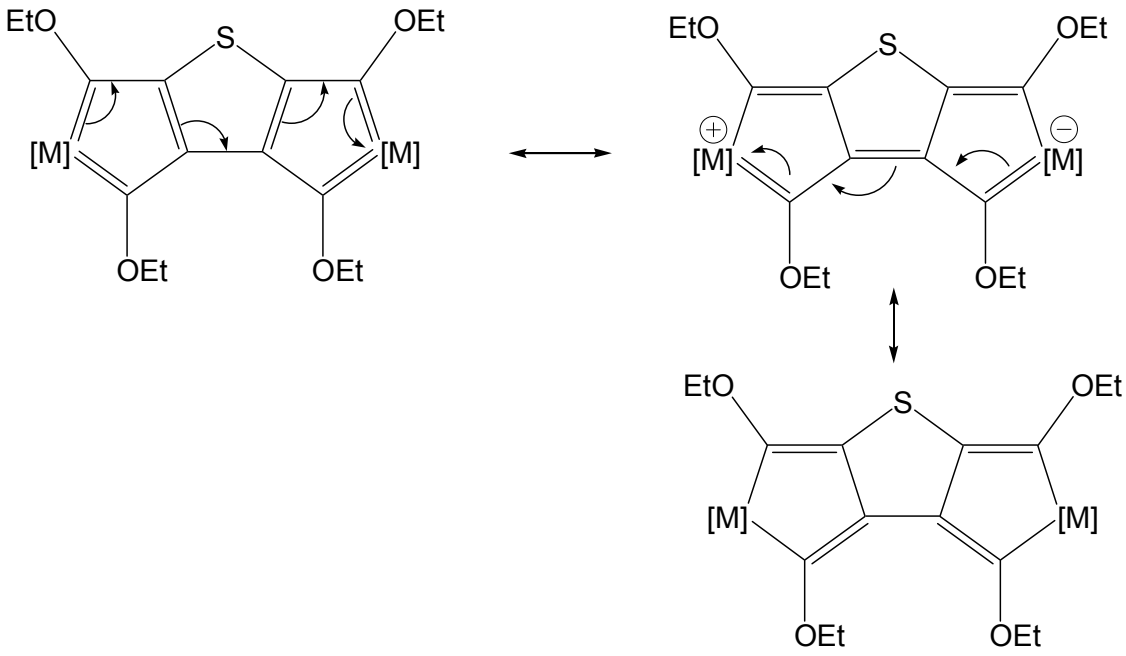

Figure 3.20: Movement of charge through the condensed rings. M=Cr(CO)$_4$ (B6) , W(CO)$_4$, (B7).

Resolution of the spectrum of complex **B7** was increased by using deuterated benzene and the individual quartet signals for the methylene protons could be resolved completely (Figure 3.21).

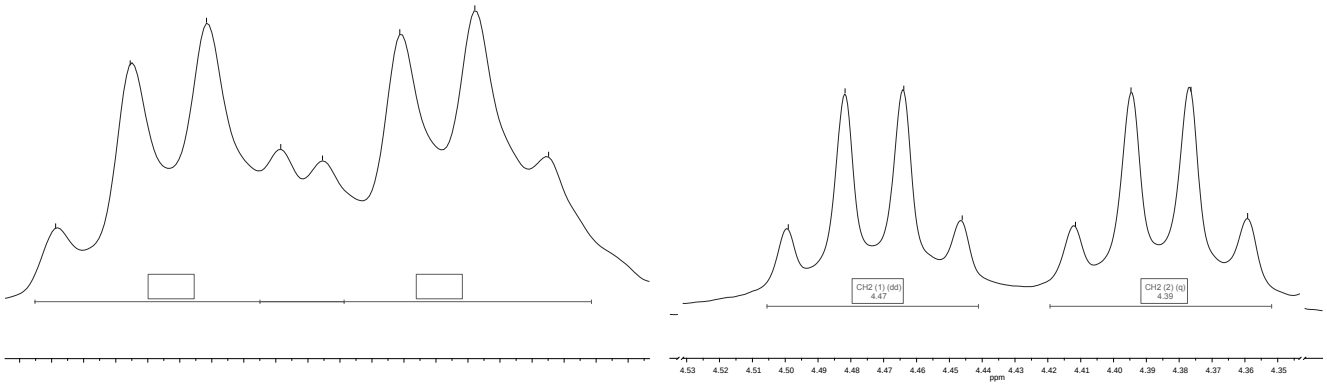

I II

Figure 3.21: ^{1}H-NMR spectra B6 of the ethoxy CH$_2$ resonance in I CDCl$_3$ and II C$_6$D$_6$.

Similar values were obtained when one carbene metal substituent was oxidized. The upfield shift of the proton resonance of the ethyl ester group was indicative of the decreased backdonation of the substituents to stabilize the central carbon atom as in the case of the carbene carbon atom.

Elucidation of byproducts from the reaction synthesis of B7

Byproducts formed during the synthesis of complex **B2** and **B3** were mainly due to the lithium halogen exchange equilibrium and consequent hydrolysis [10] of the lithiated complex. Not all the halogens were exchanged and the difference in activation energy of the respective carbon atoms allowed for exchange between the atoms already substituted on the ring. Consequently, the lithium atoms were replaced with hydrogens to produce the kinetic products and not the thermodynamic products. Protons next to the electron withdrawing fragments and in the 5-position were deshielded and those in position 4 were shielded. From this, there were eight possible monocarbene complexes of which six could positively be identified (Figure 3.22). From known chemical shift values of $[Cr\{C(OEt)C_4H_3S\}(CO)_5]$[26], complex VIII was assigned. Only complex VIII displayed J_3 and J_4 coupling and the resonances correspond to the chemical shift of proton positions H3, 4 and 5 of the 2-thienylcarbene ligand. From the influence of the position of the halogen on the bromine ring, it was possible to differentiate between the remaining monocarbene complexes. The dibromothiophene monocarbene complex has three possible analogues (II, III and IV), with the proton on the 3, 4 or 5 position.

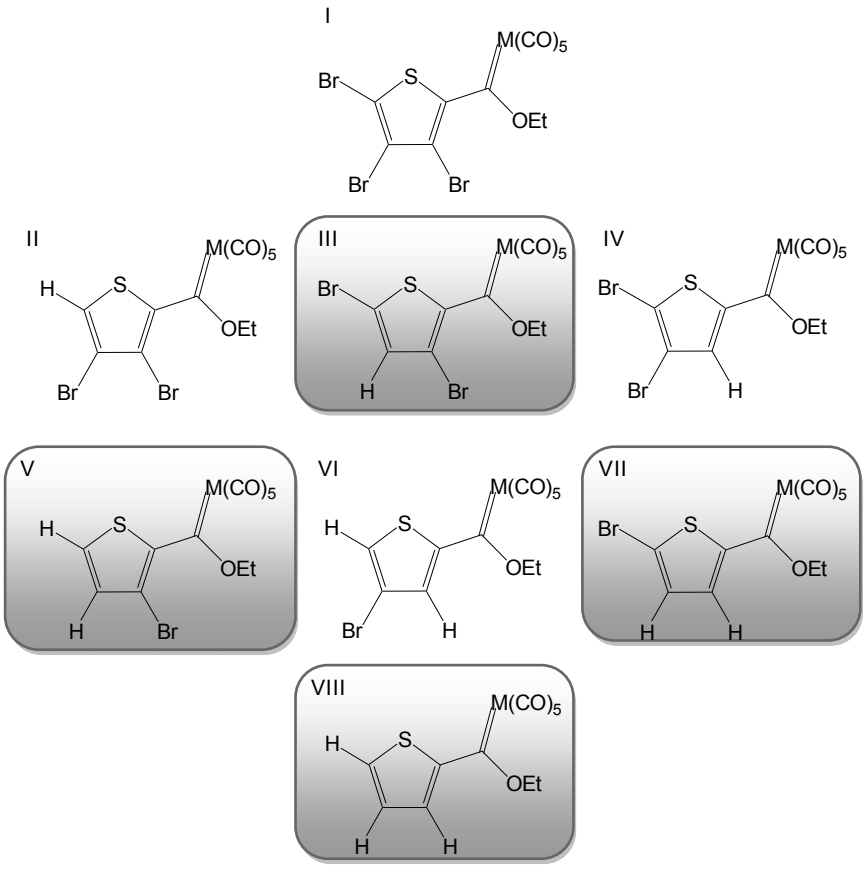

Figure 3.22: Possible kinetic and thermodynamic byproducts from the synthesis of B6 and B7 seven using 2,3,4,5-tetrabromothiophene as starting material.

From Table 3.6, a singlet at 7.76 ppm corresponded to a proton chemical shift at the 5 position considering the influence of both substituents. A chemical shift downfield would correspond to the proton on the 3 position (next to the carbene) and a shift upfield would correspond to the 4 position. A small singlet was observed at 6.76 ppm, which was attributed to complex III. Because of the activation of the 5 position, the 3,5 and 4,5-dibromo monocarbene complex analogues were kinetically unfavourable.

Table 3.6: ^{1}H-NMR spectral data of the byproducts from the synthesis of B6.

Assignments	Complexes									
	Chemical shift (δ) and coupling constant (*J*, Hz) (CD_3Cl)									
Proton	**H3**		**H4**		**H5**		$O\mathbf{CH_2}CH_3$		$OCH_2\mathbf{CH_3}$	
Complex	δ	*J*	δ	*J*	δ	*J*	δ	*J*	δ	*J*
I							4.88 (q)	7.1	1.59 (t)	7.1
II					7.74 (s)		4.91 (q)	7.0	1.66 (t)	7.0
V			7.16 (d)	5.1	7.71 (d)	5.3	5.04 (q)	7.1	1.75 (t)	7.1
VI	7.89 (d)	1.4			7.68 (d)	1.4	4.99 (q)	7.1	1.61 (t)	7.1
VII			7.27	5.3			5.00 (q)	7.1	1.66 (t)	7.1
VIII	8.17 (dd)	4.1 1.1	7.20 (2d)	4.1 5.0	7.82 (dd)	4.1 1.1	5.05 (q)	7.1	1.75 (t)	7.1

The chemical shift of the protons of free thiophene at position 5 compared to 2,3,4-tribromothiophene was 0.20 ppm downfield[31]. The shift recorded, indicated the deshielding of the proton by the presence of the combined electron negative bromine atoms and the carbene ligand. The recorded proton spectrum of 3-bromothiophene showed three doublets, (H2) 7.02, (H4) 6.85 (*J* = 3.18) and (H5) 6.98 ppm (*J* = 4.86)[32]. The downfield shift of complex V (H5, δ 7.71 and H4 δ 7.16, with the carbene metal substituent on the two position and the halogen on the 3 position, also showed the polarization of electron density towards the thienyl substituents. The degree of electron pull of the bromine fragment was much less than that of the carbene metal fragment when compared to complex **B1-3**. In contrast, complex VI has protons on position 3 and 5 recorded as 7.71 and 7.16 ppm respectively. From the coupling

[31] K. Takahashi, T. Sone, Y. Matsuki, G. Hazato, *Bull. Chem. Soc. Jpn.,***1965**, *38*, 1041
[32]H.J. Jakobsen, J.A. Nielsen, *J. Magn. Reson.,* **1969**, *1*, 393

constant J_4 = 1.4 Hz it was clear that these were not adjacent protons. Similarly the 2,4-dibromothiophene shows a coupling constant close in range to complex VI, J = 1.65 Hz[31].

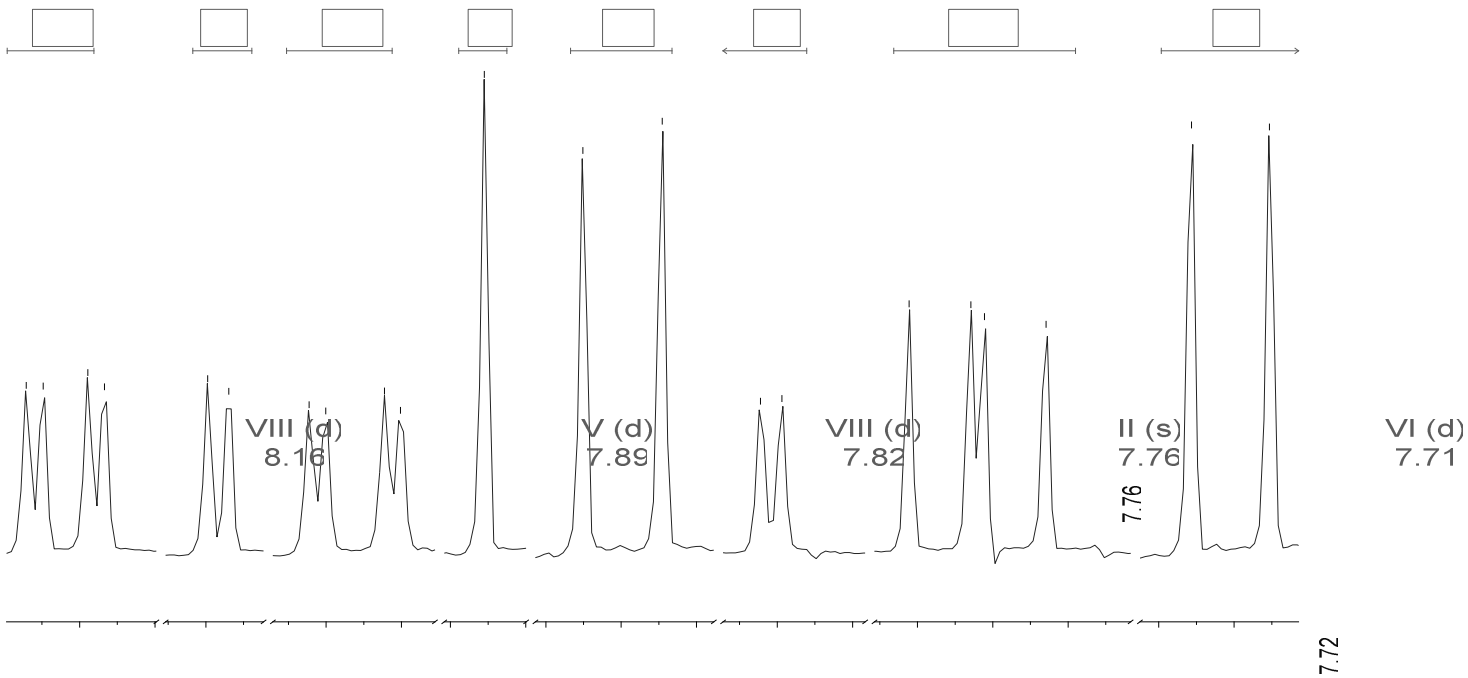

Figure 3.23: ^{1}H-NMR spectrum of the monocarbene byproducts showing the aromatic proton resonances.

The H3 resonance of complex VII could not be positively assigned, although six distinct quartet and triplet signals were observed and assigned (Figure 3.23). Based on peak intensities it was assumed that it overlaps the H3 signal of complex VIII. Complex V was assigned by two resonances (doublet) with J_3 coupling and the chemical shift correspond to protons in position 4 and 5. The carbene substituent ethoxy protons were assigned using the coupling constants, integration and the number of halogen substituents. Less π–donation from the ring will result in a larger contribution of the metal and ethoxy substituent on the carbene carbon. Thus deshielding the ethoxy protons. Complex VIII has no bromine substituents and along with the integration, corresponded to the quartet at 5.05 ppm and triplet at 1.75 ppm. This was the overall trend except for complex V where both substituents were on one side of the ring and VI where they were on opposite sides.

^{13}C-NMR Spectroscopy

Elucidation of B1-4

The ^{13}C-NMR chemical shift for a metal complex is dependent on the local and non-local involvement of the diamagnetic and paramagnetic shielding terms, which was not true for ^{1}H-NMR[33]. Thus, determination of the degree of shielding and deshielding of a carbon atom is complex and the chemical shifts are sensitive to small changes in structure[34]. Unlike in the ^{1}H-NMR spectra the ^{13}C-NMR chemical shifts are not solvent sensitive. The ^{13}C-NMR spectral data of the synthesized complexes, **B1-3** is presented in Table 3.7. There was a clear distinction between the different environments of the carbene ligands in **B1-3**. The carbene carbon atom closest to the sulphur atom (2-position) and displayed an upfield chemical shift compared to the carbene carbon atom in the 3-position. This was also reflected in the resonances of the metal carbonyl carbons of **B1** and the methylene carbons of the ethoxy substituents of **B1** and **B2**. In each case, **B1-4**, the *ipso*-carbons on the thiophene ring was shifted downfield, which was also seen for the 2,5-biscarbene chromium and tungsten complexes where the C2 and C5 *ipso*-carbons were at 157.7 and 162.6 ppm for the chromium analogue and 137.1 and 137.2 ppm for the tungsten analogue respectively[30]. Likewise the carbene chelate complex coordinated to the chromium tricarbonyl fragment (**B4** (Figure 3.24, II)) also showed the downfield shift of the C2 and C3 carbons compared to complex **B1** (Figure 3.24, I) along with the characteristic tricarbonyl shift at 232.8 ppm.

[33] A. Saika, C.P. Slichter, *J. Am. Chem. Phys.*, **1954**, *22,* 26
[34] A. Hafner, L.S. Hegedus, G. de Weck, B. Hawkins, K.H. Dötz. *J. Am. Chem. Soc*., **1988**, *110*, 8413

Table 3.7: ^{13}C-NMR data of B1-4.

Assignments	Complex				
	Chemical Shift (δ)				
Carbon atom	B1 (C_6D_6)	B1 ($CDCl_3$)	B2 ($CDCl_3$)	B3 (C_6D_6)	B4 (C_6D_6)
C$_{carbene\ a}$	312.3	312.3	319.9	283.3	312.0
C$_{carbene\ b}$	321.1	321.0	323.8	313.9	
M(**C**O)$_4$ *trans*	227.9	227.2	217.1	201.1	222.4
M(**C**O)$_4$ *cis*		217.5	212.9	191.0	216.4
O**C$_a$H$_2$**CH$_3$			78.8	78.4	94.3
O**C$_b$H$_2$**CH$_3$	76.9	76.6	78.6	78.6	91.8
OCH$_2$**C$_a$H$_3$**	14.8	15.2	15.6	14.9	14.5
OCH$_2$**C$_b$H$_3$**					14.3
C2 *ipso*	167.5	167.3	164.9	164.7	108.9
C3 *ipso*		144.9	147.5		100.7
C4	134.7	134.6	134.9	134.7	93.0
C5	116.6	116.7	117.8	117.7	97.7
Cr(**C**O)$_3$					232.8

The carbonyl carbons for each metal fragment was characteristic with little influence from the substituent. In contrast, the thienyl carbon chemical shift was influenced by the proximity to the sulphur and the presence of the carbene ligand. For complex **B1-4** the *ipso*-carbon (C2) was shifted downfield compared to the other *ipso*-carbon (C3). The influence of the ability of thiophene to stabilize the separate carbene carbons was manifested in the difference between the chemical shift values (Figure 3.14). The more shielded carbene **a** was upfield from carbene **b**.

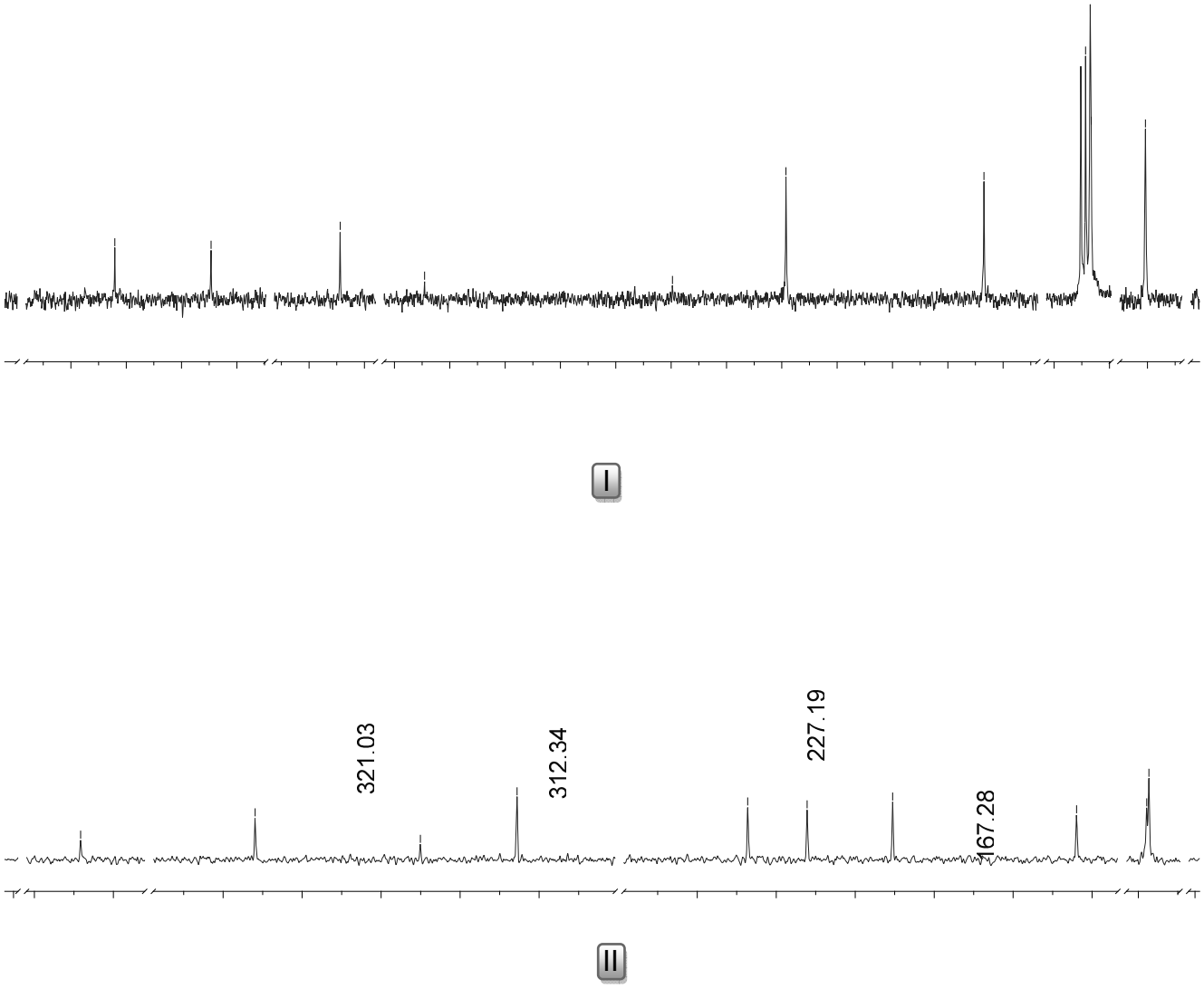

Figure 3.24: ^{13}C-NMR spectra of B1, (I) in $CDCl_3$ and B4 (II).

The carbon atom resonances of all four thienyl carbons of complex **B4** were also shifted upfield in II compared to that of complex **B1** in spectrum due to the effect of the chromium tricarbonyl fragment. Correlation spectroscopy was used to verify the influence of the substituents on the thienyl ring and the HETCOR of complex **B1** is shown in Figure 3.25.

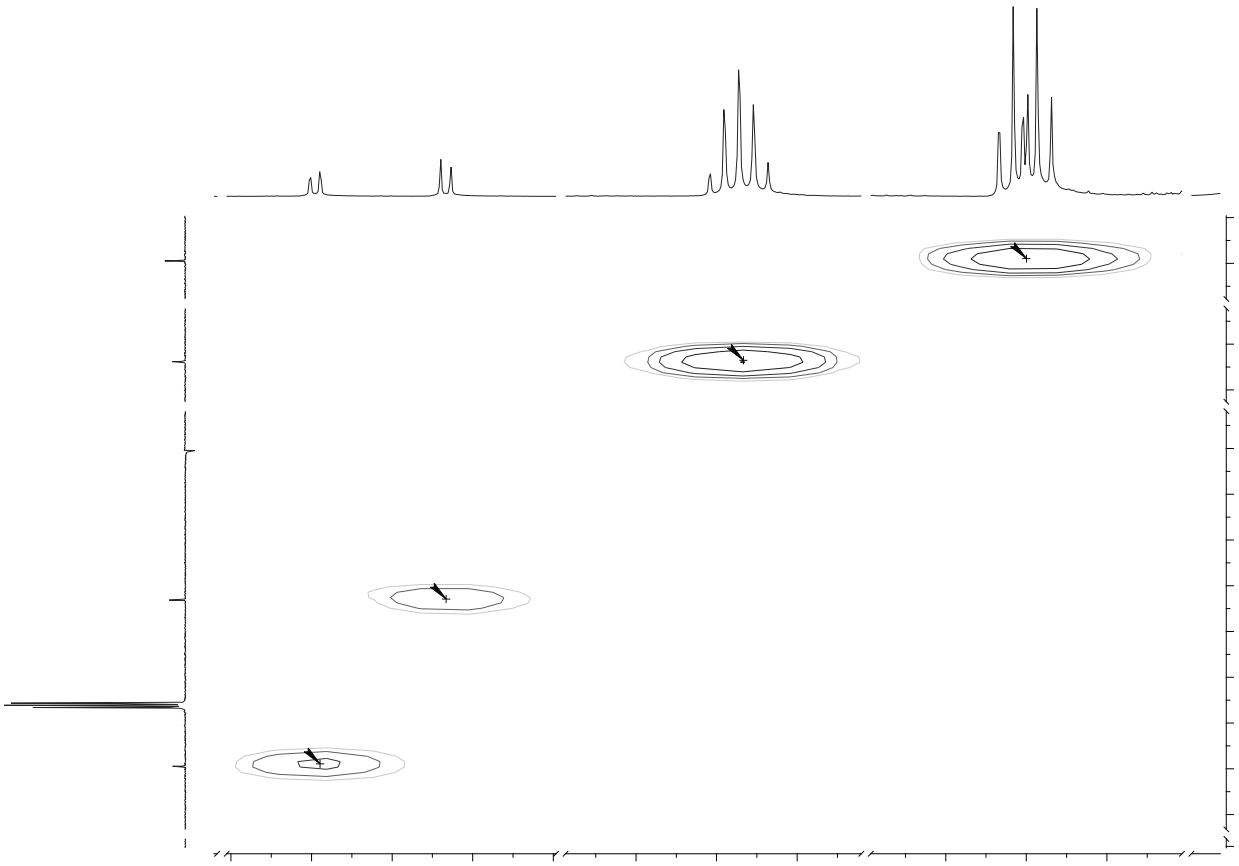

Figure 3.25: HETCOR spectrum of B1 in C_6D_6.

As seen from the correlation plot, there was a large difference in the environment of the C4 and C5 thiophene carbon atoms due to the influence of the thiophene carbon attached to the carbene carbon in position 3.

{6.43,116.45}

{6.59,134.44}

Elucidation of B5

Table 3.8: ^{13}C-NMR spectrum of B5.

Assignments	Complex
	Chemical Shift (δ)
Carbon atom	**B5 ($CDCl_3$)**
C$_{carbene}$	312.1
C$_{carbene}$	320.8
M(**C**O)$_4$ *cis*	226.9
O**CH$_2$**CH$_3$	76.8
OCH$_2$**CH$_3$**	15.0
C2 *ipso*	168.0
C3 *ipso*	166.0
C4	134.4
C5	113.9

The chemical shift pattern for the aminolysis product **B5** showed two distinct carbene signals similar to those of the starting material complex **B1**. Carbene complexes with weak donor ability such as a methyl and methoxy substituent has a large downfield shift for the carbene carbon resonance at 361.0 ppm[34], increasing the donor ability by substituting the ethoxy group of complex **B1** for a NH_2 substituent shifts has little effect and are similar to **B1**[34] (Table 3.8).

Elucidation of test reaction with 2,3,4,5-tetrabromothiophene

From the test reaction performed on tetrabromothiophene with one equivalent of BuLi the following tetrabromothiophene carbon resonances for referencing, were found in $CDCl_3$ at 110.4 and 117.1 ppm, respectively. From the reaction mixture the following values where obtained for the ethoxy substituent, CH_2 (4.97 ppm (q), J = 7.1) and CH_3 (1.64 ppm (m)). Proton signals observed in the aromatic region suggested that there was halogen-lithium exchange during the reaction. From this spectrum little information could be obtained due to broadening of the peaks. The resolution of the ^{13}C-NMR spectrum was sufficient to assign the signals to two individual complexes (Figure 3.26). There was a multitude of possibilities for the consequent replacement of the bromine with a hydrogen *via* lithiation bearing in minds both thermodynamic and kinetic products may be present. In this case only the kinetic products were observed with lithiation of the most reactive carbon atoms.

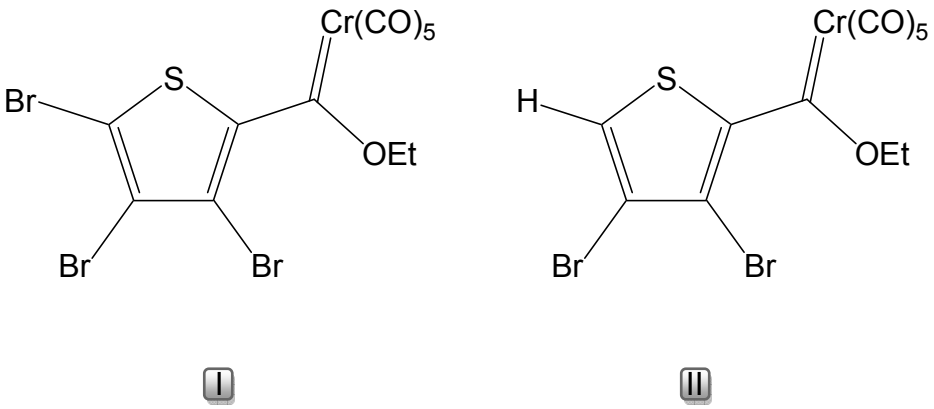

Figure 3.26: Carbene complex analogues identified for the test reaction on 2,3,4,5-tetrabromothiophene.

The bromine replacement was noticed in the ^{13}C-NMR spectrum (Figure 3.27). Looking at the thienyl carbon resonances the strong signal observed at 123.9 ppm, is characteristic of a C-H carbonyl chemical shift corresponding to structure II in Figure 3.26.

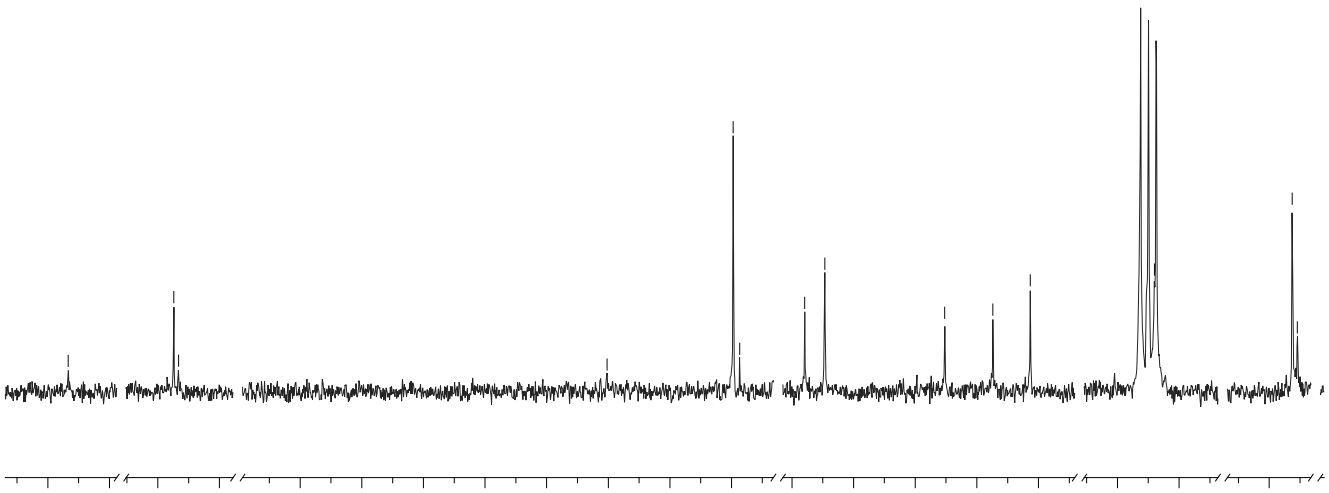

Figure 3.27: ^{13}C-NMR spectrum of monocarbene chromium complex from 2,3,4,5-tetrabromothiophene.

Considering the reported chemical shift values of 3,4-dibromothiophene [31]. The influence of the bromine atom on the carbon chemical shift value resulted in an upfield shift. The chemical shift of C2 was reported at 123.75 ppm and 113.95 ppm for C3. This corresponded well with the chemical shift of the C-H thienyl carbon atom at 123.9 ppm (Table 3.9). The chemical resonances of C3 and C4 was upfield compared to that of the C2 *ipso* carbons for both complexes. The downfield shift of the *ipso* carbon was also observed for other carbene complex derivatives reported here.

Table 3.9: ^{13}C-NMR data obtained for the test reaction of 2,3,4,5-tetrabromothiophene.

Assignments	Complex	
	Chemical Shift (δ)	
Carbon atom	I	II
C2 *ipso*	123.7	128.0
C3	117.6	116.9
C4	111.5	110.3
C5	113.04	123.9

Elucidation of B6 and B7

Table 3.10: ^{13}C-NMR data of B6 and B7.

Assignments	Complex	
	Chemical Shift (δ)	
Carbon atom	**B6*** (C_6D_6)	**B7** (C_6D_6)
C$_{carbene}$	317.4	283.7
C$_{carbene}$	325.3	317.8
M(**C**O)$_4$ *trans*	226.7	209.1
M(**C**O)$_4$ *trans*		194.8
M(**C**O)$_4$ *cis*		212.4
M(**C**O)$_4$ *cis*		195.1
O**CH$_2$**CH$_3$	77.3	79.9
O**CH$_2$**CH$_3$	76.9	81.2
OCH$_2$**CH$_3$**	15.0	14.8
OCH$_2$**CH$_3$**	14.7	14.7
C2, 5 *ipso*		165.4
C3,4 *ipso*	151.8	158.3

There was a broadening of the signals observed for the carbonyl ligands of **B6 making it difficult to assign a specific value for each*.

With two chelate rings on thiophene for the tetracarbene complexes, similar chemical shift patterns were observed to those of the carbene monochelate complexes **B1-3** in Table 3.7. There was a notable downfield shift in the carbene carbon and carbonyl resonances of both **B1** and **B2** due to the backbonding of the metal substituent to the now strained thienyl ring. This influence of all four carbene metal fragments on the ring was evident from the large downfield shift of the ring carbon resonance.

Elucidation of byproducts from the reaction synthesis of B7

From the correlation spectrum, the individual thienyl resonances were assigned to the individual thienyl carbon chemical shifts. There were eight weaker signals observed between 106.8-124.4 ppm, which were attributed to the carbon chemicals shifts of thienyl carbons with a bromine atom. There were six sets of carbonyl and ethoxy methylene (CH_2) signals observed which links to the ^{1}H-NMR spectrum of the mixture showing six methylene resonances in different environments.

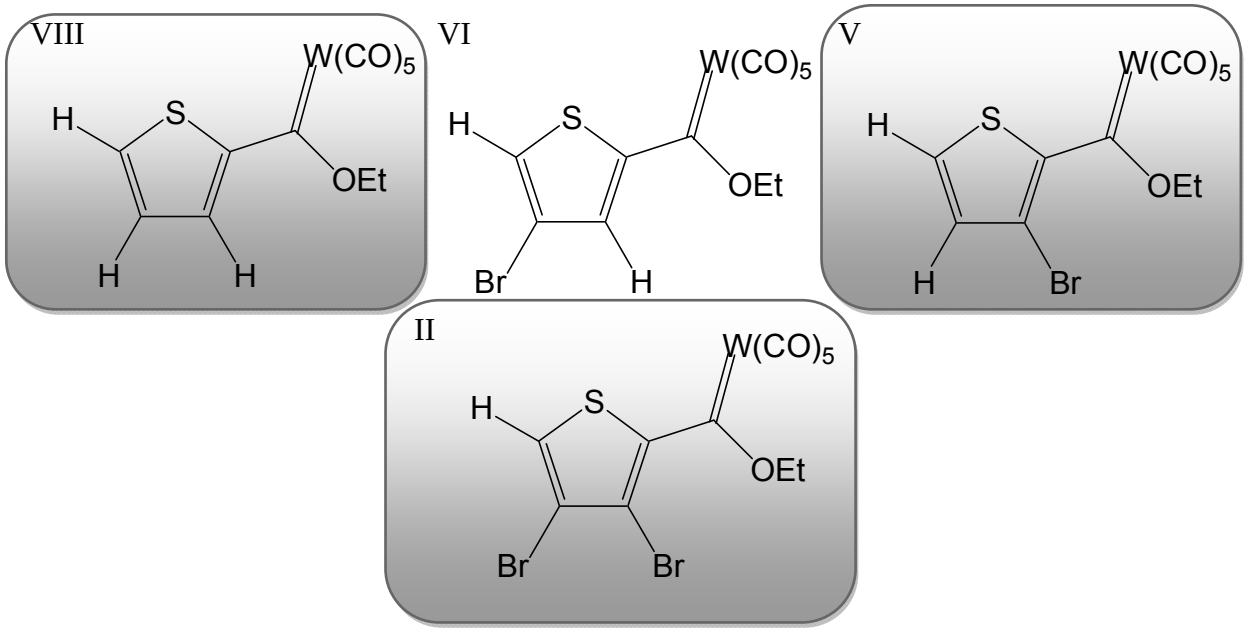

Figure 3.28: Possible kinetic and thermodynamic byproducts from the synthesis of B6 and B7 using 2,3,4,5-tetrabromothiophene as starting material.

For the ethoxy (CH_3) chemical shifts, only five signals were observed (14.7-15.5 ppm). Contrary to the ^{1}H-NMR spectroscopy, ^{13}C-NMR spectroscopy was not as sensitive to change in environment but from the spectrum observed, the difference in environment was clear due to the resolution and range of the individual peaks. The *cis*-carbonyls were observed between δ 197.6 and δ 196.8 as six individual signals of different intensities, but only 3 *trans*-carbonyl

signals were observed (202.5 – 202.0 ppm). The six *ipso*-carbon signals attached to the carbene carbon could all be assigned. The absence of one methylene CH_3 resonance may be due to overlap of the signals, as these signals are characteristically strong.

IR-Spectroscopy

Assignments of B1-3 and B6 and B7

Table 3.11: Infrared data obtained of B1-3, B5-7 in hexane.

Assignments		Complex					
		Stretching vibrational Frequency (vCO, cm^{-1})					
		B1	**B2**	**B3**	**B5**	**B6**	**B7**
$M(CO)_4$	**$A_1^{(1)}$**	2018 (s)	2025 (s)	2018 (s)	2017 (s)	2008 (s)	2017 (vs)
	$A_1^{(2)}$	1959 (vs)	1952 (vs)	1959 (vs)	1958 (vs)	1960 (vs)	1961 (vs)
	B_1	1946 (s)	1942 (s)	1948 (s)	1934 (vs)	1947 (vs)	1945 (vs)
	B_2	1895 (s)	1888 (s)	1896 (s)	1894 (s)	1890 (s)	1897 (s)

The wavelength pattern observed for the number of carbonyl ligands and the symmetry of the specific complex are characteristic[35]. For $ML_2(CO)_4$ there are four distinct bands observed for complex **B1**, **B2** and **B3** (Table 3.11). The $A_1^{(2)}$ and B_1 band often show overlap but the B band is of higher intensity compared to the $A_1^{(2)}$[36]. These values correspond to that observed

[35] Ch. Elschenbroich, A. Salzer, *Organometallics: a concise introduction 2nd edition.* **1992**, Verlagsgesellschaft, New York
[36] [36] P.S. Braterman, *Metal carbonyl spectra,* **1975**, Academic Press, New York, USA

for the mononuclear biscarbene complexes reported by Fischer[37] (Table 3.12). The substituents on the carbene metal carbon influence the *trans* carbonyl wavelength and it was shifted.

Table 3.12: Selected IR data of the carbonyl stretches for I [M{1,2-C(OEt)C_6H_4C(COEt)}$(CO)_4$] and II [M{C(OEt)CH(Ph)CH(Ph)C(OEt)}$(CO)_4$] in DCM.

Assignments		Complex				
		Stretching vibrational Frequency (vCO, cm^{-1})				
		I			II	
		Cr	W	Mo	Cr	W
$M(CO)_4$	$A_1^{(1)}$	2018	2032	2035	2010	2030
	$A_1^{(2)}$	1953	1957	1963	1945	1955
	B_1	1947	1947	1953	1935	1945
	B_2	1898	1896	1905	1900	1900

Substituents with better donor ability, such as the NH_2 substituent on the carbene carbon atom in complex **B5,** decreased the backbonding from the carbene carbon atom to the metal and the metal interaction with the *trans* carbonyl group was more prominent[34]. This interaction leads to a longer wavelength shift. This shift was usually smaller if the other substituent was an aryl group.

[37] E.O. Fischer, W. Röll, N.H.T. Huy, K. Ackermann, *Chem. Ber.,* **1982**, *115*, 2951.

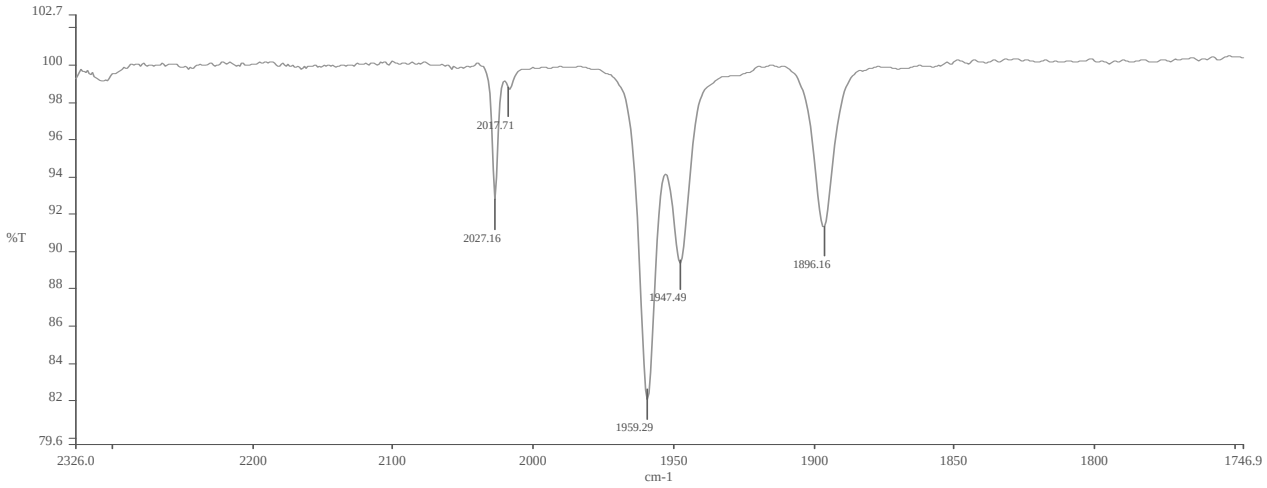

Figure 3.29: Infrared spectrum of the v_{CO} region obtained for B3.

UV spectra

Assignments of B1 and B2, and B6 and B7

The UV spectrum of thiophene in solution displayed two bands at 215 and 231nm[38]. Substituents on the thiophene ring will influence the position of the bands. Thiophene is electron excessive and in π-conjugation with the metal through the carbene ligand. The NMR data and crystal structure determinations show polarization of the electron density through the complex. The UV-spectra of **B1**, **B2** and **B6** and **B7** were representative of the complexes and display bands in 3 regions (Table 3.13). Strong ligand based absorption bands between 285 and 295 nm were observed. The second regions between 330-390 nm displayed intense

[38] [38] C. Crause, PhD Thesis, *Synthesis and application of carbene complexes with heteroaromatic substituents*, **2004,** University of Pretoria.

bands which belong to the thiophene, based π-π* transitions. The bands were shifted to represent lower energy (wavelength) and relate to transitions, which indicated interaction of the metal carbene π-system with that of the thiophene substituents. The absorption bands at the lowest energy (above 500 nm) was assigned to the metal-d carbene-p charge transfer transitions. The value of this transition is closely related to the colour of the complex. From literature, the three defined regions of Fischer metal-carbene complexes are between 300-350nm for the ligand field transition, 350-450 nm for the spin-allowed and ligand field absorption and around 500nm for the metal-ligand charge transfer (MLTC)[39]. These regions correspond well with those obtained for the carbene chelate complexes **B1**, **B2**, **B6** and **B7** summarized in the table below and also to values observed for the mononuclear biscarbene complexes reported by Fischer and Ackermann[40] (Table 3.14) in benzene. The electronic spectra of the chromium and tungsten carbene complexes show similar absorption with four absorption bands[34].

Table 3.13: UV data obtained of B1, B2, B6 and B7.

Assignments	Complex			
	UV-absorption λ (nm)			
Complex	**B1**	**B2**	**B6**	**B7**
d-p (M→L)	597 (0.14)	574 (0.1)	514 (0.11)	587 (0.1)
	513 (0.17)			518 (0.06)
π-π*(thiophene)		392 (0.62)	418 (0.14)	
	376 (0.63)	335 (0.45)	3.89 (0.14)	371 (0.59)
Ligand absorptions	290 (0.82)	290 (0.700	287 (0.33)	291 (0.29)

[39] (a) M.L. Lage, I. Fernández, M.J. Mancheño, M.A. Sierra, *Inorg. Chem.*, **2008**, *46*, 5253
(b) L.S. Hegedus, *Tetrahedron* **1997**, *53*, 4105
[40] E.O. Fischer, W. Röll, N.H.T. Huy, K. Ackermann, *Chem. Ber.,* **1982**, *115*, 2951.

Table 3.14: Reported UV-absorption data for [M{η^2-1,2(*o*-C_6H_4)C$(OEt)_2$} $(CO)_4$] where M = Cr, W and Mo[40].

Assignments	Complex		
	UV-absorption λ (nm)		
Complex	Cr	W	Mo
M (d-2p)	540 (0.031)	562 (0.029)	547 (0.03)
π-π*(benzene)	397 (0.30)	412 (0.092)	403 (0.26)
	322 (0.087)	313 (0.073)	320 (0.083)
Ligand absorptions	244 (0.054)	236 (0.44)	247 (0.52)

Reported molecular orbital calculations[41] show that the excitation of an electron from the HOMO to the LUMO was attributed to the metal-to-ligand charge transfer and the ligand absorption band was ascribed to the metal centred LUMO+1. In the figure below was the graphical representation of the highest occupied and lowest unoccupied orbitals of complex **B1**, **B2** and **B7** in Figure 3.30, Figure 3.31 and Figure 3.32.

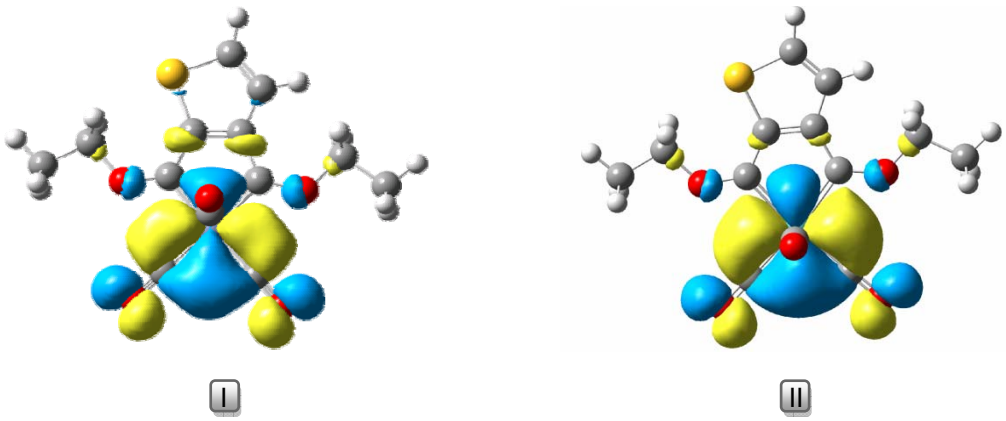

Figure 3.30: Graphic representation of the HOMO of B1 (I) and B2 (II).

The transfer of electrons between these orbitals resulted in the shift observed in absorption. However, the study of the exact orbitals between which the electron transfer takes place was

[41] (a) T.J. Block, R.F. Fenske, C.P. Casey, *J. Am. Chem. Soc.* **1976**,*98*, 441
(b) H. Nakatsuji, J. Uskio, T. Yonezawa, *J. Am. Chem. Soc.***1983**, *105*, 426
(c) H.C. Foley, L.M. Strubinger, T.S. Targos, G.L. Geoffroy, *J. Am. Chem. Soc.* **1983**, *105*, 3064.

not an aim of this study. The technique was applied to a series of such complexes as **B1**, **B2** and **B3** as a qualitative addition to the study to give insight into the electronic structure. The HOMO and LUMO orbitals would indicate the sites of highest reactivity.

Figure 3.31: Graphic representation of the LUMO orbitals of B1 (I) and B2 (II).

There is a correlation between the position of the bands and the substitution on the carbene carbon ligand. Change in colour and intensities were reported[39] when the carbene substituent was changed from a methyl to a π-donating group causing a strong red shift effect. The colour reported for **B1** and **B2** was a deep blue and **B7** was a very intense purple appearing almost black. Thus the change in colour due to the different substituent corresponded to the change in intensity and the transfer of electrons between the HOMO and LUMO orbitals. Attack with nucleophiles will occur predominantly on the carbene carbon atoms of **B1**, **B2** and **B7** as shown by LUMO orbitals.

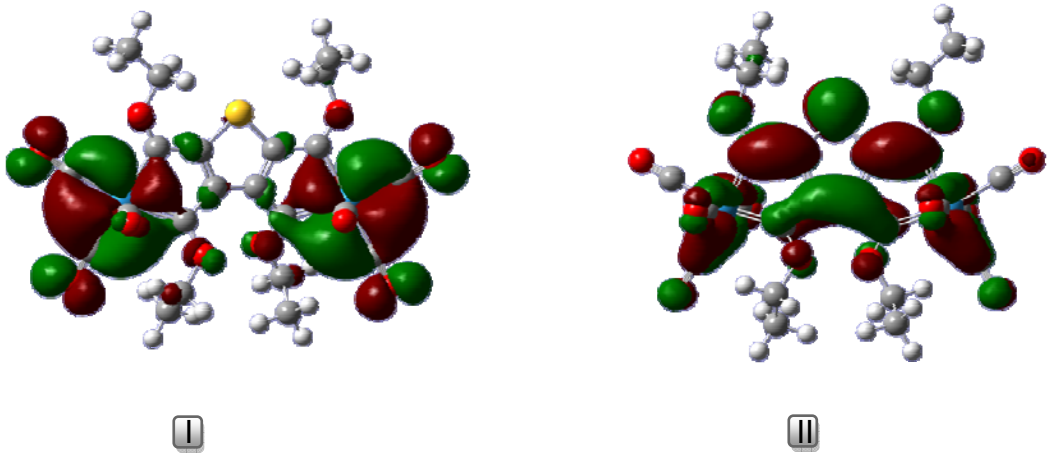

Figure 3.32: Graphic representation of the HOMO (I) and LUMO(II) orbitals of B7.

Mass Spectrometry

Mass data of B2, B4 and B7

Mass spectrum analyses were done on representative complexes **B2**, **B4** and **B7** and is reported in the table below.

Table 3.15: Selected *m/z* peaks identified for B2, B4 and B7.

Complex	*m/z* (Intensity)
B2	n.o. [M^+], 480 (0.8) [M^+-4CO], 424 (0.03) [M^+-$(CO/C_2H_4)_2$]
B4	n.o [M^+], 412 (0.3) [M^+-3(CO)], 384 (0.5), [M^+-4CO], 356 (0.1), [M^+-5CO], 328 (0.08), [M^+-6CO],
B7	900 (0.3), [M^+], 872 (0.4), [M^+-CO], 844 (0.3), [M^+-2CO], 817 (0.2), [M^+-3CO], 790 (0.4) [M^+-4CO], 762 (0.2), [M^+-5CO], 731 (0.3), [M^+-6CO], 706 (0.25), [M^+-7CO], 675 (0.2) [M^+-CO/C_2H_4]

The most labile ligands on the carbene chelate complexes were the metal carbonyl ligands and the isotope cluster of the peaks are at intervals of *m/z*-values that showed the chronological fragmentation of the carbonyl ligands. There was no molecular ion peak observed for complex **B1**. The sequential loss of four carbonyl ligands were observed followed by the loss of two additional CO or C_2H_4 fragments. The initial loss of three carbonyls for complex **B4** corresponded to this tricarbonyl metal fragment followed by the carbonyl fragments of the carbene ligand. The fragmentation of the labile carbonyls of complex **B7** was chronological and 7 carbonyl isotope clusters were observed followed by a fragment that could either represent the C_2H_4 fragment from the methylene or another carbonyl. The mass spectrum of **B7** is given below showing all seven carbonyl isotope clusters.

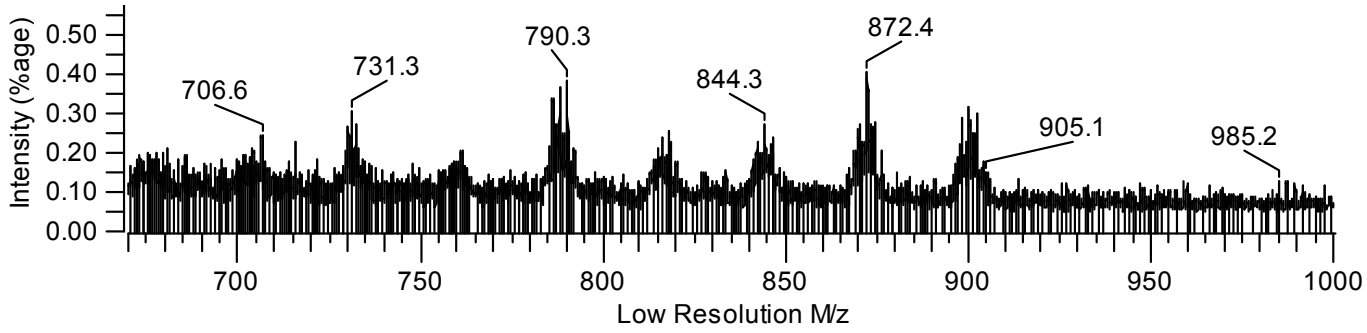

Figure 3.33: Mass spectrum obtained of B7.

X-Ray Diffraction

From single crystal X-ray diffraction studies the structures of complexes **B1**, **B3**, **B5** and **B7** were obtained and confirmed correlations drawn from the spectroscopic measurements. These are presented with their atoms numbered below as ORTEP[42]+POV[43]-Ray pictures in Figure 3.34 (**B1** and **B3**), Figure 3.36 (**B5**) and Figure 3.37 (**B7**), respectively. Hydrogens were subjectively assigned as round spheres whereas other atoms were displayed as ellipsoids showing the anisotropic displacement. Crystal structures of the isomorphous complexes, **B2** and **B3** were obtained and are displayed as ORTEP+POV-Ray pictures (Figure 3.35). The C4 hydrogen atom was replaced with a lithium atom and these complexes are referred to as **B2a** and **B3a**. Other graphical representations of the crystal structure were obtained using Mercury software[44].

[42] L.J. Farrugia, *J. Appl. Crystallogr.,* **1997**, *30,* 565
[43] The POV-Ray Team 2004, <http//www.pov-ray.org/download/>
[44] (a) F. H. Allen, *Acta Cryst.*, **2002**, 380, Mercury CSD 2.0 2002
(b)J. van de Streek, *Acta Cryst.*, **2006**, 567, Mercury visualization 2006

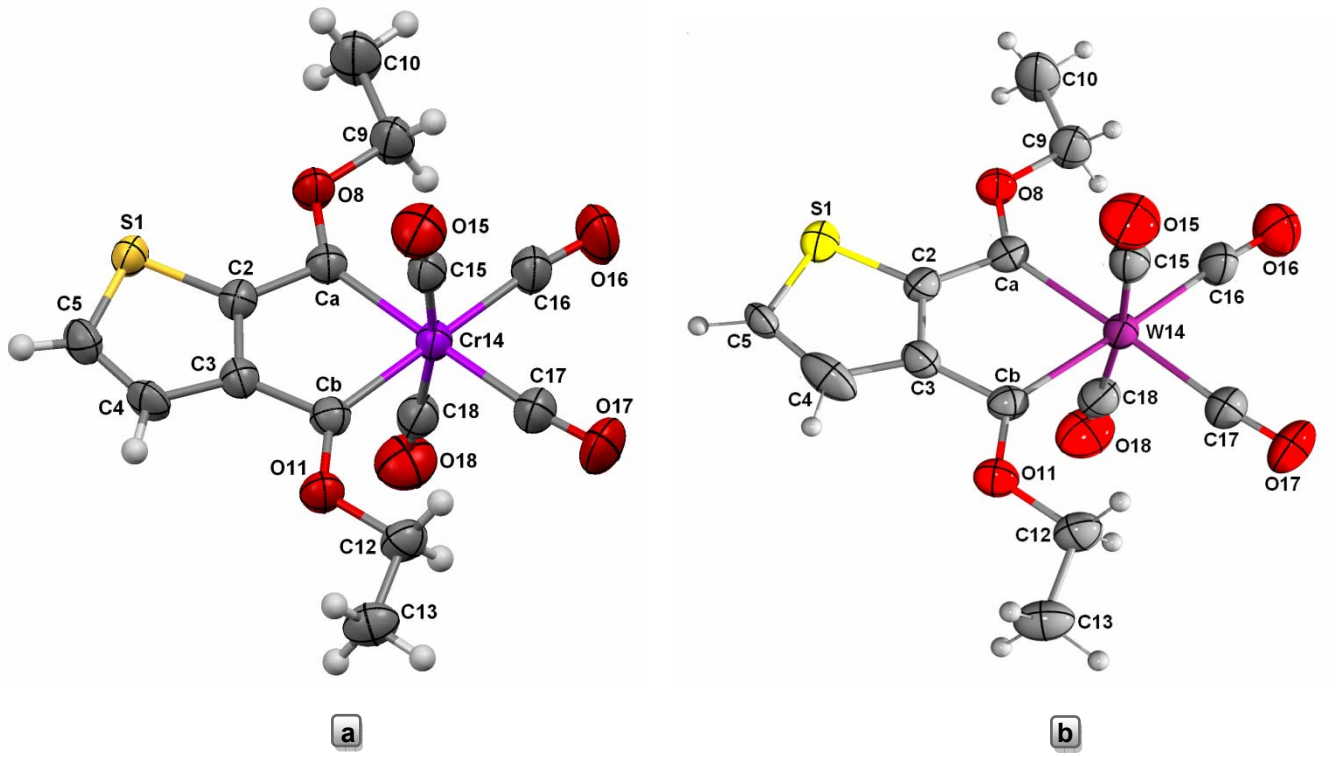

Figure 3.34: ORTEP+ POV-Ray representation of B1 (a) and B3 (b).

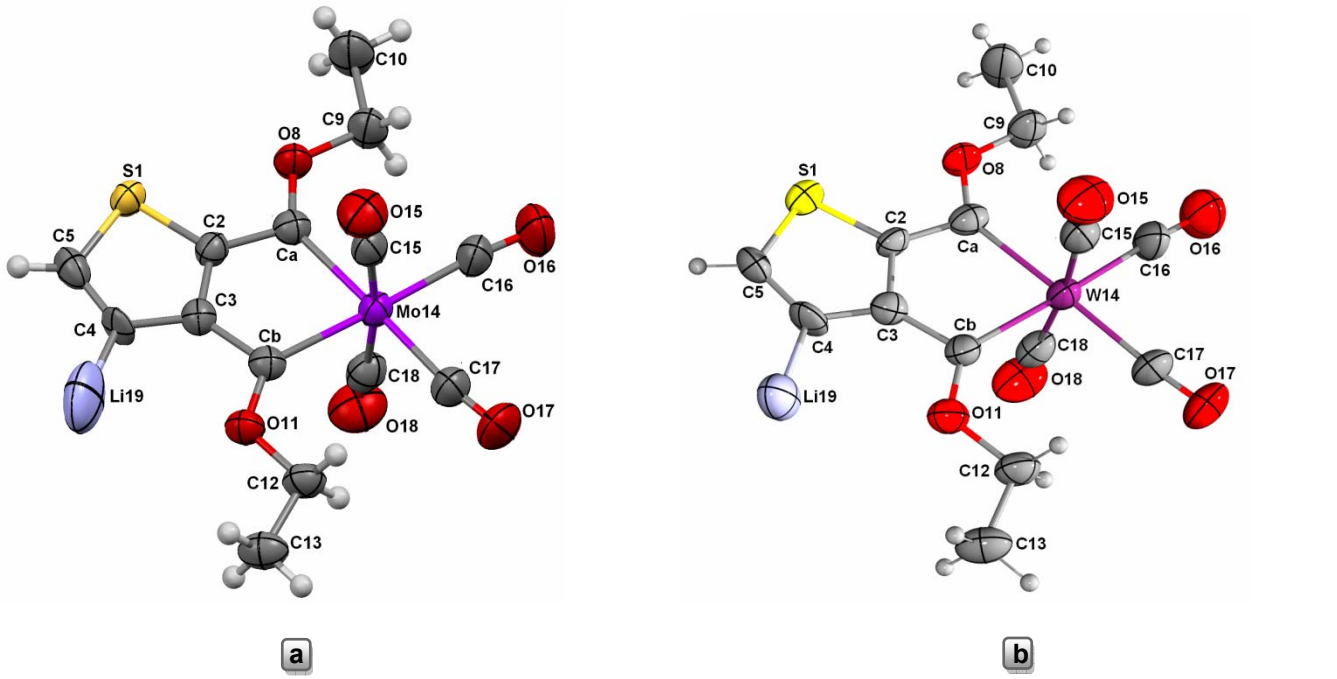

Figure 3.35: ORTEP+POV-Ray representation of isomorphous for B2a (a) and B3a (b).

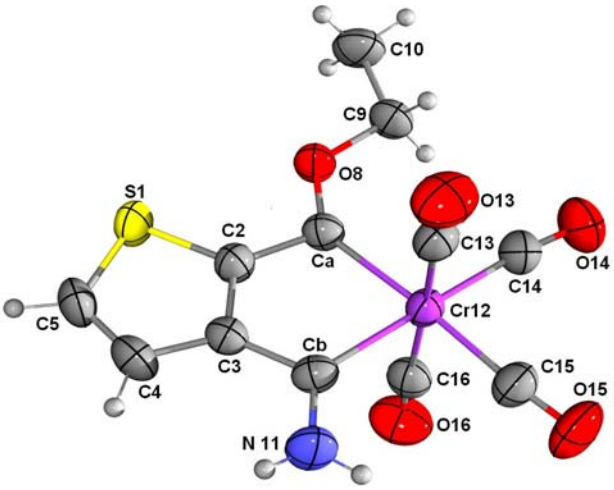

Figure 3.36: ORTEP, POV-Ray representation of B5.

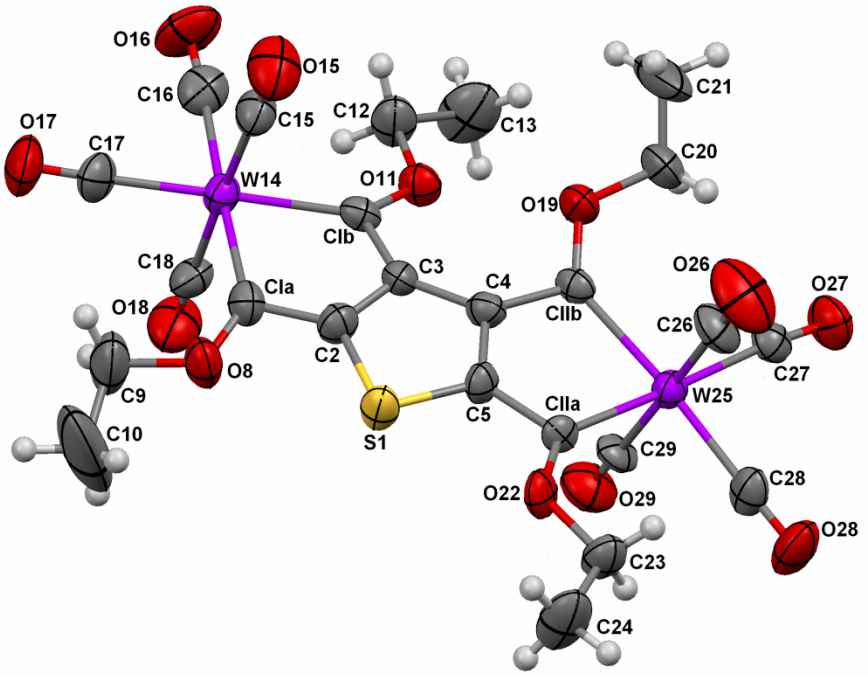

Figure 3.37: ORTEP+ POV-Ray representation of B7.

The six ligands were found in a distorted octahedral arrangement around the metal with the two carbene ligands as part of a five membered chelate ring and hence coordinated *cis* to

each other. This was observed for all six chelate structures. Note, the bisecting the conjugated ring system is designated as area **a** and **b** with respect to the carbene carbons and with **a** always on the side of the sulphur atom. The thiophene and chelate rings are coplanar with the ethoxy substituents slightly above and below the plane of the condensed ring system for **B1**, **B2a**, **B3**, **B3a** and **B5**. Figure 3.38 shows a plane through the thiophene substituent of **B1**, **B2a**, **B3** and **B5**. For **B7** the ethoxy substituents were almost in plane with the conjugated ring system on the side of the sulphur atom. On the other side the space is more crowded and the ethoxy substituents are orientated with one above and one below the plane of the rings. The condensed ring system of **B7** showed two of the rings were coplanar and the third with the metal fragment pushed above the plane.

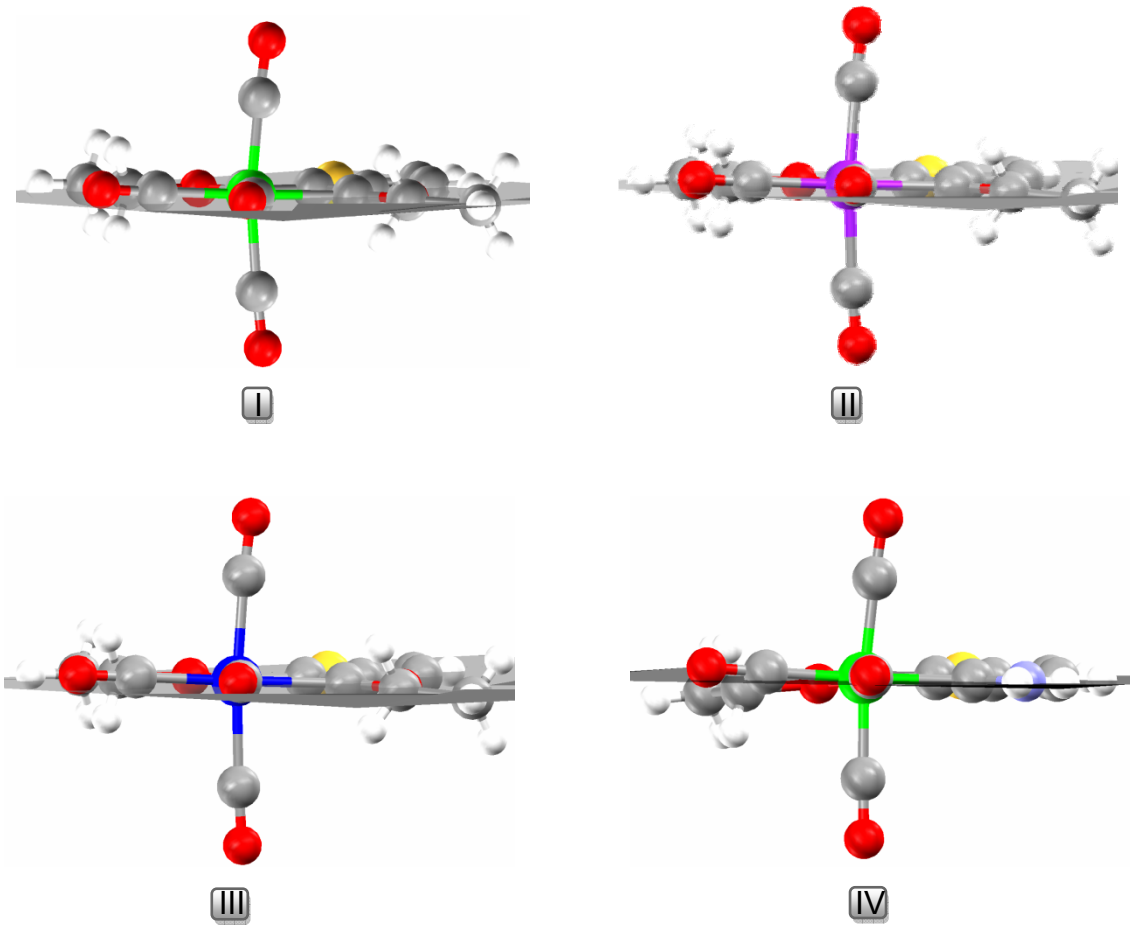

Figure 3.38: View along the axis of the *trans* carbonyl ligand of carbene$_a$ of B1 (I), B2a (II), B3 (III) and B5 (IV).

The greatest distortion in the complexes are the two carbonyls not in plane with the carbenes. These carbonyls bend towards the chelate ring for **B1**, **B2a**, **B3**, **B3a** and **B5**. This is unlike for [M(carbene)$(CO)_5$] complexes where the axial carbonyl ligands bend away from the carbene ligand. This was ascribed to the uneven interaction of one p-orbital of the carbene ligand with two π*-orbitals of the carbonyl ligands. The $C_{carbene}$-M-$C_{carbene}$ angle of the chelate ring is 81.70(7)º **B1** and 78.22(13)º **B3** respectively which have a distortion effect on the other angles of the metal octahedron. These are greater than 90º like the angles in the equatorial plane between the chelate ring ligands and the adjacent carbonyl ligands, the effect described above for the axial carbonyl ligands being greater than 90º on the other side of the carbene ligands and the chelate ring. The same observations were made for **B5** and **B7**. The $C_{carbene}$-M-$C_{carbene}$ bond angle is 80.86 (8) **B5** and 77.5 (4) and 77.8 (4) for **B7**. The smaller bond angle for **B7** was due to the presence of four carbene ligands on one thienyl ring, which resulted in greater strain and competition between the individual ligands for stabilization. The ethoxy substituents on the carbene are orientated with the lone pair electrons of the oxygen towards the thienyl substituent. Orientation of the oxygen substituents is relative and dependent on the steric factors [45,46]. For **B1**, **B3**, **B2a**, **B3a**, **B5** and **B7** the ethoxy groups were in the *anti* orientation with respect to the thienyl ring. Contrary to pentacarbonyl carbene complexes the oxygen of the ethoxy ligand was eclipsed with the 'carbonyl wall' this orientated the lone pairs of the oxygen towards the sulphur atom for **B1**, **B2a**, **B3**, **B3a** and **B5**. Notably the steric strain of the ethoxy substituents on the other side of the sulphur atom in complex **B7** resulted in the distortion of the $C_{carbene}$-C_{thp} bond attached to C_3 and C_4 (C_{Ib}-C_3-C_4-C_{IIb}, 15(3)º). The ethoxy groups moved with the metal carbonyl fragment to remain eclipsed. Selected bond lengths of complexes **B1**, **B3**, **B2a** and **B3a** are reported in Table 3.16 and bond angles in Table 3.17. Bond angles and lengths for complex **B5** are presented in Table 3.19 and Table 3.20 and those for complex **B7** in Table 3.21 and Table 3.22 in that order. Detailed tables of bond lengths and bond angles are available in the appendices.

[45] C.G. Kreiter, E.O.Fischer, *Angew. Chem. Int. Ed. Engl.,* **1969,** *8,* 761
[46] (a) D.M. Andrada, M.E. Zoloff Michoff, I.Fernández, A.M. Granados, M.A. Sierra, *Organometallics,* **2007,** *26,* 5854
(b) I. Fernández, F.P. Cossío, A. Arrieta, B. Lecea, M.J. Mancheño, M.A. Sierra, *Organometallics*, **2004**, *23*, 1065

Selected data of B1-3

Table 3.16: Selected bond distances for complexes B1, B2a, B3 and B3a.

Bond		Space Group			
		$P2_{1c}$			
		Bond distance (Å)			
		B1	**B2a**	**B3**	**B3a**
Carbene a	$C_{carbene}$-M	2.0591(17)	2.158(3)	2.164(4)	2.173(7)
	$C_{carbene}$-C_{thp}	1.479(2)	1.454(4)	1.450(5)	1.458(10)
	$C_{carbene}$-OEt	1.330(2)	1.304(4)	1.317(4)	1.308(8)
	M-CO_{trans}	1.903(2)	2.003(4)	2.017(4)	2.028(8)
	M-CO_{cis}	1.933(2)	2.048(5)	2.056(5)	2.046(10)
Carbene b	$C_{carbene}$-M	2.0636(18)	2.152(3)	2.176(3)	2.155(7)
	$C_{carbene}$-C_{thp}	1.478(2)	1.460(4)	1.452(5)	1.436(10)
	$C_{carbene}$-OEt	1.331(2)	1.311(4)	1.304(4)	1.320(9)
	M-CO_{trans}	1.913(2)	1.997(4)	2.009(4)	2.002(9)
	M-CO_{cis}	1.936(2)	2.049(4)	2.067(5)	2.061(10)
Thiophene	S-C_2	1.739(3)	1.725(4)	1.703(4)	1.715(6)
	C_2-C_3	1.389(3)	1.378(5)	1.385(6)	1.391(10)
	C_3-C_4	1.431(6)	1.396(8)	1.395(9)	1.390(10)
	C_4-C_5	1.382(7)	1.366(8)	1.391(9)	1.383(9)
	C_5-S	1.726(7)	1.713(8)	1.734(9)	1.724(10)

Comparison of bond lenghts in Table 3.16 revealed similar bond lengths for the $C_{carbene}$-M distances (C_a and C_b) on complex **B1** and **B3**. These bonds were shorter than the corresponding M-C_a and M-C_b bonds of **B2a** and **B3a** respectively due to the size effect of

different metals. The lengthening of the M-$C_{carbene}$ bond distances may also be attributed to the minimilization of interaction of the ethoxy substituent with the 'carbonyl wall'. Because the ethoxy group eclipsed the 'carbonyl wall' the interaction was greater compared to a staggered conformation[46]. Notably the distance in **B1** was the same as those reported for the Cr-$C_{carbene}$ distances of 2.05 Å of chromium[methoxy(phenyl)carbene]pentacarbonyl [47*,45].

Table 3.17: Selected bond angles of B1 and B3.

Bond Angles		Space Group			
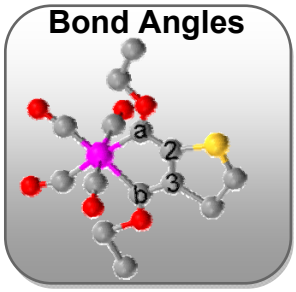		$P2_{1/c}$			
		Bond angles (°)			
		B1		**B3**	
		a	**b**	**a**	**b**
Carbene	M-$C_{carbene}$-C_{thp}	112.49(12)	113.29(12)	113.4(2)	112.8(2)
	EtO-$C_{carbene}$-C_{thp}	109.78(14)	109.32(15)	109.9(3)	110.7(3)
	$C_{carbene\ a}$–M-$C_{carbene\ b}$	81.70(7)		78.22(13)	
	CO_{trans}-M-CO_{trans}	79.82(9)		82.60(18)	
	$C_{carbene\ a}$-M-CO_{trans}	99.03(8)		99.71(16)	
	$C_{carbene\ b}$-M-CO_{trans}	99.46(8)		99.47(15)	
Thiophene	S-C_2-C_3	114.08(14)		114.4(3)	
	C_2-C_3-C_4	109.0(3)		107.1(6)	
	C_3-C_4-C_5	114.9(5)		119.5(9)	
	C_4-C_5-S	111.4(6)		106.2(8)	
	C_5-S-C_2	90.7(3)		92.8(4)	

[47] C.G. Kreiter, E.O. Fischer, *Angew. Chem. Int. Ed. Engl.*, **1969,** *8,* 761
* Standard bond deviation not reported.

Table 3.18: Selected bond angles of B2a and B3a.

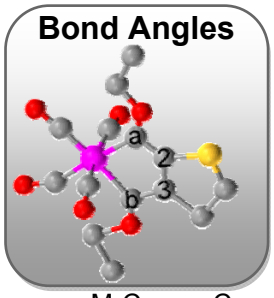

		Space Group			
		$P2_{1/c}$			
		Bond angles (º)			
		B2a		B3a	
		A	b	a	b
Carbene	M-$C_{carbene}$-C_{thp}	112.2(2)	113.1(2)	112.3(5)	114.0(5)
	EtO- $C_{carbene}$-C_{thp}	110.1(3)	109.6(3)	110.7(6)	109.0(6)
	$C_{carbene\ a}$-M-CO_{trans}	99.46(14)		99.7(3)	
	$C_{carbene\ b}$-M-CO_{trans}	99.29(14)		99.7(3)	
	$C_{carbene\ a}$–M-$C_{carbene\ b}$	78.93(12)		78.3(3)	
	CO_{trans}-M-CO_{trans}	92.57(16)		82.3(4)	
Thiophene	S-C_2-C_3	114.2(2)		114.8(5)	
	C_2-C_3-C_4	108.7(5)		107.7(8)	
	C_3-C_4-C_5	115.8(7)		117.2(11)	
	C_4-C_5-S	111.1(7)		109.4(10)	
	C_5-S-C_2	90.2(4)		90.8(6)	

The distortion in the bond angles of the *trans* carbonyls in the plane of the chelate ring is ascribed to the geometrical constraints caused by the ring. The bond angles $C_{carbene\ a}$-M-$C_{carbene\ b}$ of **B1** was 81.70(7)º, correspondingly the bond angles of complex **B2a**, **B3** and **B3a** were also less than 90º, 78.93(12)º, 78.22 (13)º and 78.3(3)º of the thiophene ring respectively. Surprisingly these angles were smaller than the recorded C_5-S-C_2 bond angles. These bond angles were 90.7(3)º, 90.2(4)º, 92.8(4)º and 90.8(6)º for **B1**, **B2a**, **B3** and **B3a** respectively.

Selected data of B5

Table 3.19: Selected bond lengths for complex B5.

Bond		Space Group	
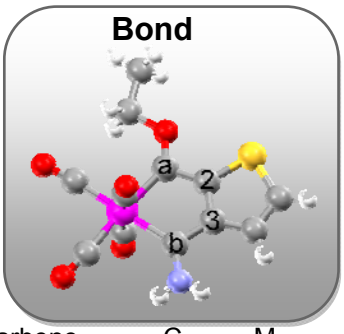		P1	
		Bond distance (Å)	
		B5	
		a (R=OEt)	**b (R=NH_2)**
Carbene	$C_{carbene}$-M	2.042(2)	2.064(2)
	$C_{carbene}$-C_{thp}	1.451(3)	1.456(3)
	$C_{carbene}$-R	1.313(2)	1.309(3)
	M-CO_{trans}	1.866(2)	1.866(2)
	M-CO_{cis}	1.897(2)	1.887(2)
Thiophene	S-C_2	1.711(3)	
	C_2-C_3	1.375(3)	
	C_3-C_4	1.389(7)	
	C_4-C_5	1.353(8)	
	C_5-S	1.711(6)	

The π-interaction of the metal to the carbene carbon, C_b, with the nitrogen substituent is expected to be less than that of carbene carbon C_a, in spite of the fact that nitrogen is bigger than oxygen the $C_{carbene}$-N distance is the same as the $C_{carbene}$-O distance. This indicates greater π-bonding from the nitrogen compound to the oxygen with the carbene carbon with the oxygen substituent. The contribution of the thienyl ring is the same but the nitrogen atom is a better π-donor than the oxygen atom. The bond lengths of the $C_{carbene}$–O bond for complex **B1** were 1.330(2) Å and 1.331(2) Å and complex **B2a**, **B3**, **B3a** and **B7** showed related bond lengths. These were expected to be different from that of **B5** due to the better backbonding

from the NH_2 substituent but this is not the case. From this, one could conclude that the carbene ligands of the chelate in **B5** acts independently with little overall effect to the complex and the general insensitivity of the M-$C_{carbene}$ bond distances are ascribed to the geometrical constraints imparted on the chelate ring.

Table 3.20: Selected bond angles of B5.

Bond Angles		Space Group
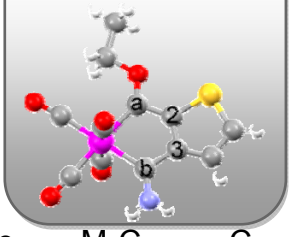		P1
		Bond Angles (Å)
		B5
Carbene $_a$	M-$C_{carbene}$-C_{thp}	112.67(14)
	EtO- $C_{carbene}$-C_{thp}	108.92(17)
	$C_{carbene}$-M-CO_{trans}	99.20(9)
Carbene $_b$	M-$C_{carbene}$-C_{thp}	130.36(17)
	NH_2- $C_{carbene}$-C_{thp}	115.9(2)
	$C_{carbene}$-M-CO_{trans}	94.74(9)
	$C_{carbene\ a}$–M-$C_{carbene\ b}$	80.86(8)
	CO_{trans}-M-CO_{trans}	85.20(11)
Thiophene	S-C_2-C_3	112.64(16)
	C_2-C_3-C_4	111.5(5)
	C_3-C_4-C_5	113.0(7)
	C_4-C_5-S	112.8(5)
	C_5-S-C_2	90.1(3)

The bond angles M-$C_{carbene}$-C_{thp} deviate notably for carbene **a** (112.67(14)º) and **b** (130.26(17)º). This coincides with the difference in bond distances for the carbene to the respective heteroatoms, $C_{carbene}$-OEt (1.313(2) Å and $C_{carbene}$-NH_2 (1.309(3) Å). The shorter $C_{carbene}$-NH_2 bond distance results in a decreased backbonding from the metal and thus an increase in the bond angle. This observation supports the fact that the substitution of both

ethoxy groups resulted in the increase of both M-$C_{carbene}$ bonds and the M-$C_{carbene}$-C_{thp} bond angles so much so that the metal fragment was expelled from the system. This was experimentally observed when both ethoxy substituents were aminolyzed.

Selected data of B7

Table 3.21: Selected bond lengths of B7.

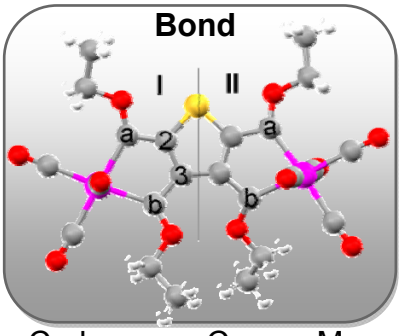

Space Group		P1	
Bond distance (Å)		B7	
		I	II
Carbene a	$C_{carbene}$-M	2.134(10)	2.134(12)
	$C_{carbene}$-C_{thp}	1.474(14)	1.451(16)
	$C_{carbene}$-O	1.290(12)	1.330(14)
	M-CO_{trans}	2.022(13)	2.000(13)
	M-CO_{cis}	2.050(15)	2.047(15)
Carbene b	$C_{carbene}$-M	2.189(11)	2.186(11)
	$C_{carbene}$-C_{thp}	1.469(15)	1.498(14)
	$C_{carbene}$-O	1.310(13)	1.312(12)
	M-CO_{trans}	2.022(13)	2.046(15)
	M-CO_{cis}	2.064(13)	2.057(15)
Thiophene	S-C_2	1.708(11)	
	C_2-C_3	1.405(15)	
	C_3-C_4	1.445(15)	
	C_4-C_5	1.379(15)	
	C_5-S	1.737(11)	

Table 3.22: Selected bond angles of B7.

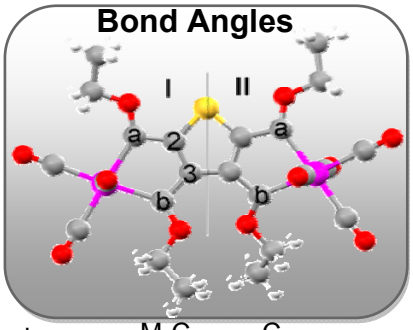

Space Group					
		P1			
Bond distance (Å)					
		B7			
		I		II	
		a	b	a	b
Carbene	M-$C_{carbene}$-C_{thp}	113.1(7)	114.2(7)	112.8(8)	114.4(7)
	EtO- $C_{carbene}$-C_{thp}	108.3(9)	110.6(9)	107.6(10)	109.3(9)
	$C_{carbene\ a}$–M-$C_{carbene\ b}$	77.5(4)		77.8(4)	
	$C_{carbene\ a}$-M-CO_{trans}	98.4(4)		98.6(5)	
	$C_{carbene\ b}$-M-CO_{trans}	99.7(4)		99.8(5)	
	CO_{trans}-M-CO_{trans}	83.3(5)		83.9(6)	
Thiophene	S-C_2-C_3	114.9(8)			
	C_2-C_3-C_4	109.2(9)			
	C_3-C_4-C_5	112.5(9)			
	C_4-C_5-S	113.2(8)			
	C_5-S-C_2	90.0(5)			

Symmetry axis C_2 divides the molecule in two halves, I and II. The corresponding bond distances are the same for the two halves. The most notable difference of the structure are the conformation of the ethoxy substituents which is very open on the sulphur side of the thiophene ring, but are very crowded on the opposite side. As a result the metal-carbene distances differ significantly in the chelate rings. The W-$C_{carbene}$ bond distances of complex **B3**, **B3a** and **B7** are similar to the tungsten biscarbene complex on the 2 and 5 position of the furan ring reported by Crause[48]. These distances were reported as 2.166(6) Å and 2.139(6) Å. The respective distance in complex **B3**, **B3a** and **B7** were 2.164(4) Å C_a and 2.176(3) Å C_b for complex **B3**, 2.173(7) C_a and 2.155(7) Å C_b and complex **B7** 2.134(10) Å C_{la}, 2.189(11) Å C_{lb},

[48] C. Crause, H. Görls, S. Lotz, *Dalton Trans*., **2005**, 1649-1657

2.134(12) Å C_{IIa} and 2.186(11) Å C_{IIb}. The decreases in the M-$C_{carbene}$ bond length correlates with an increase in the M-CO_{trans} bond length[49]. The decreases in the M-CO_{trans} bond lengths compared the M-CO_{cis} distances are the most prominent for complex **B1**, **B2a**, **B3**, **B3a** and **B5**. These bond lengths in complex **B7** show contribution from both *cis* and *trans* carbonyl ligands. The presence of four electron withdrawing groups on the thienyl moiety having to share the available electron density equally, resulted in an increase in the metal contribution to stabilize the carbene carbon. Thus the contribution of the carbonyl groups are to adapt to this requirement of the metal to stabilize the structure.

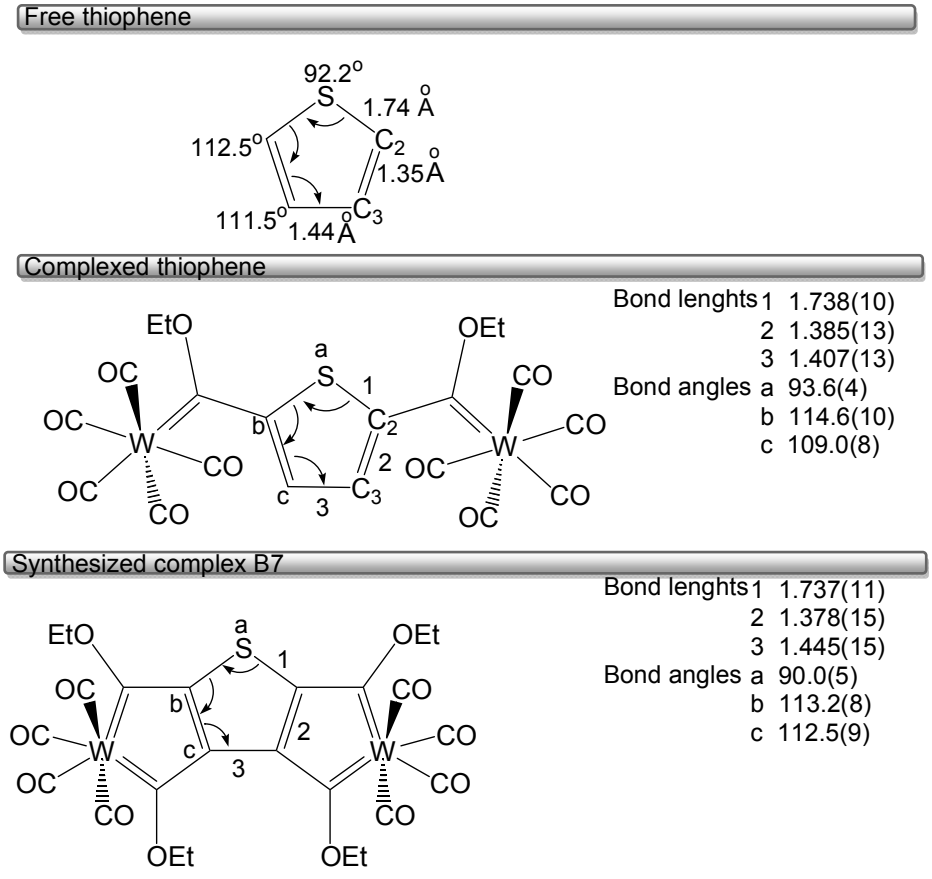

Figure 3.39: Selected thienyl bond lengths for free thiophene[50]*, a thienyl biscarbene complex [30]and B7.

[49] (a) K. Kitaura, K. Morokuma, *Int. J. Quant. Chem.*, **1976,** *10,* 325,
(b) T. Ziegler, A. Rauk, *Theor. Chim.*, **1977,** *46,* 1
(c) T. Ziegler, A. Rauk, *Inorg. Chem.*, **1979,** *18,* 1558
(d) T. Ziegler, A. Rauk, *Inorg. Chem.*, **1979,** *18,* 1755

[50] N.D. Epiotis, W.R. Cherry, F. Bernardi, W.J. Hehre, *J. Am. Chem. Soc.*, **1976,** *98,* 4361

* The standard deviation of the thiophene bond lengths and angles were not reported in the reference article

The influence of the carbene metal fragments on the thiophene ring of B7 compared to 2,5-thiophene metal biscarbene complex is shown in Figure 3.39. The symmetrical 2,5-thiophene metal biscarbene complex reflected an almost equal contribution from the thienyl ring to both carbene metal fragments. The influence of the tetracarbene ligand on the thienyl ring bond distances are the same in the biscarbene complex. The greatest discrepancy between free thiophene, the biscarbene complex and **B7** are the bond angles of the thiophene ring. Example: the C_2-S-C_5 bond angle for free thiophene (92.2º) and the biscarbene complex (93.6(4)º) are the same but differ significantly from that of **B7** (90.0(5)º). The molecule is strained due to the conjugated ring system resulting in the deviation of the bond angles. The non-symmetrical carbene complexes **B1**, **B3**, and **B5** can not be compared with these symmetrical systems. Nevertheless, the influence of the respective carbene monochelate complexes, **B1**, **B3**, and **B5** on the thienyl ring was compared. There was a disparity in the C_3-C_4 bond distances of **B1** (1.431(6) Å) **B3**, (1.395(9) Å) and **B5** (1.389(7) Å) compared to free thiophene (1.44 Å), which is ascribe to the constrained geometry, bond delocalization and the donor ability of the thienyl moiety.

Packing

Complex **B1** show five distinctive hydrogen oxygen interactions (Figure 3.40). The molecules pack in an alternating pattern creating a grid-like pattern of chains linked by intermolecular interactions. Complex **B3** (Figure 3.40) showed the same interaction and packing pattern to that of **B1**. The molecules of **B1** and **B3** interacted in an alternating pattern to form chains. These interact with the next chain orientated in the reverse direction (Figure 3.40 (b), Figure 3.41 (b)). It was also observed that the hydrogen of an ethoxy group from a neighbouring molecule was in close proximity (2.88 Å) to the C_2-C_3 double bond of thienyl ring for complex **B1** and (2.793 Å) **B2**.

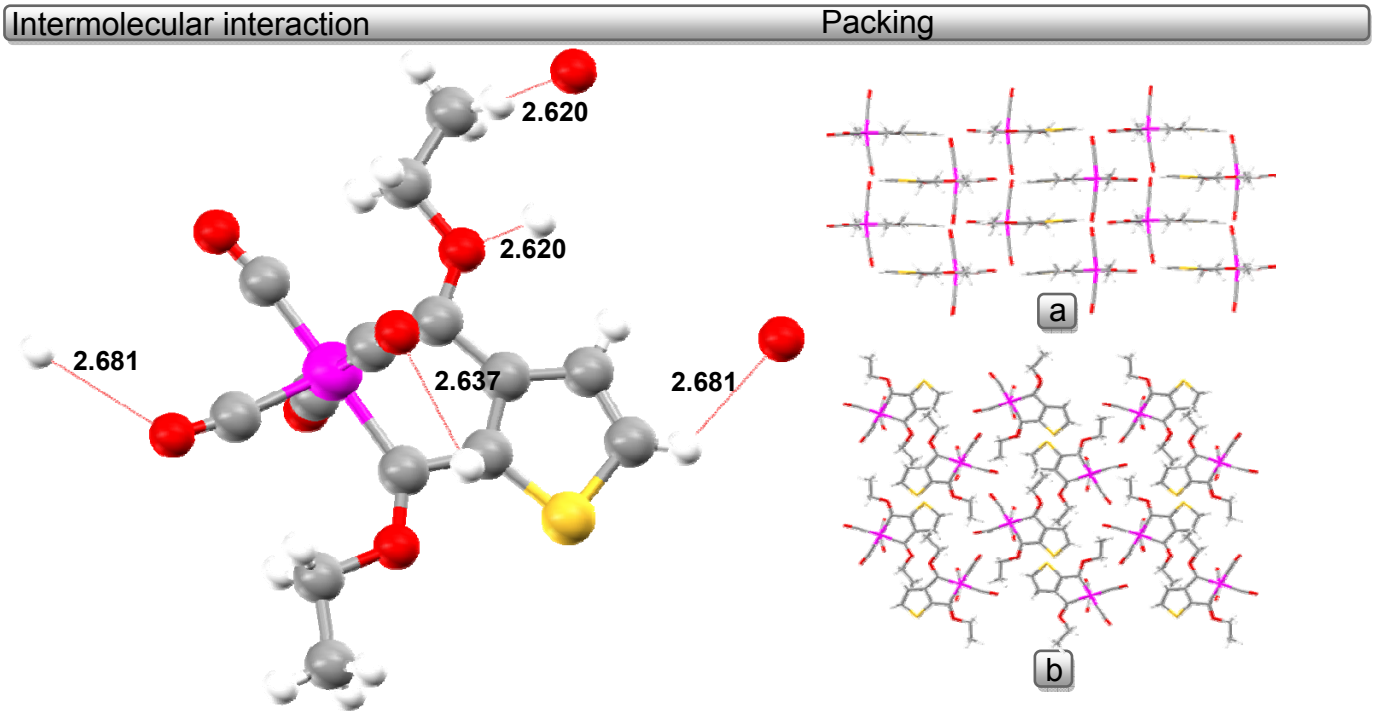

Figure 3.40: Intermolecular interaction and packing of B1.

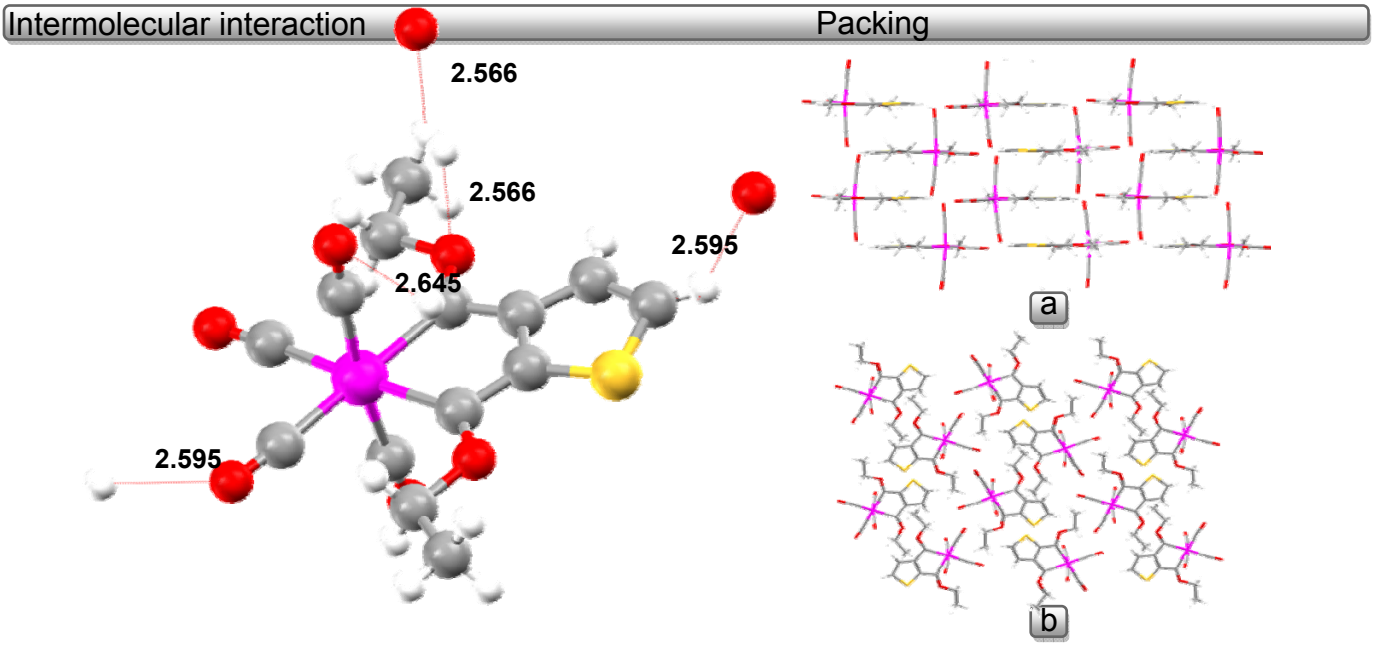

Figure 3.41 : Intermolecular interaction and packing of B3 (a and b).

The presence of the unreacted lithium placed on position C4 of the thienyl substituent in complex **B2a** and **B3a**, allowed for interaction with the oxygen on a *cis* carbonyl of a neighbouring molecule (Figure 3.42).

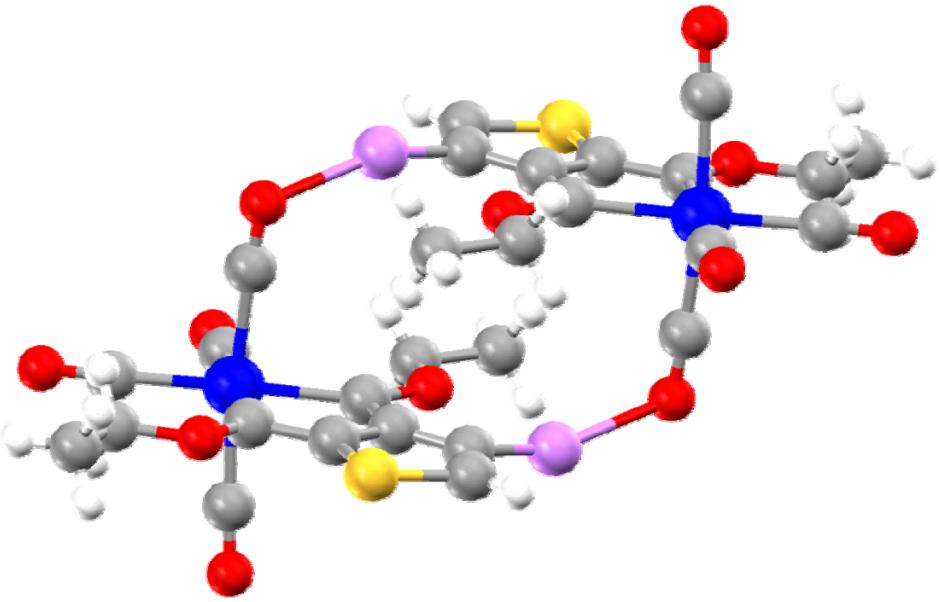

Figure 3.42: Precursor complex of B3a displaying a lithium atom on position C4 with $P2_1$ space group.

Hydrolysis of the lithium atom from trace amount of water present results in the formation of the target material. Synthesis of complex **B1** with 2-bromothiophene did not result in this complex forming but it was observed for the synthesis using 2,3,4,5-tetrabromothiophene (**B2a** and **B3a**). The lithium atom links the two separate chelate complexes to make a square. The plane of the thienyl and chelate carbonyl fragment was not parallel as with complex **B1** and **B3**. There were hydrogen interactions with two molecules below and one above. One molecule interacts with five other molecules in its surrounding to form a pattern consisted of a chain linked to the neighbouring chains, which were inverted relative to the first chain. In turn the squares stack on top and beside one another to form a grid-like pattern (Figure 3.43 (a)). The interaction of this molecule with neighbouring molecules allowed for packing in a network-like grid *via* hydrogen bonding. Hydrogen interactions on each side of the molecule kept the structure rigid.

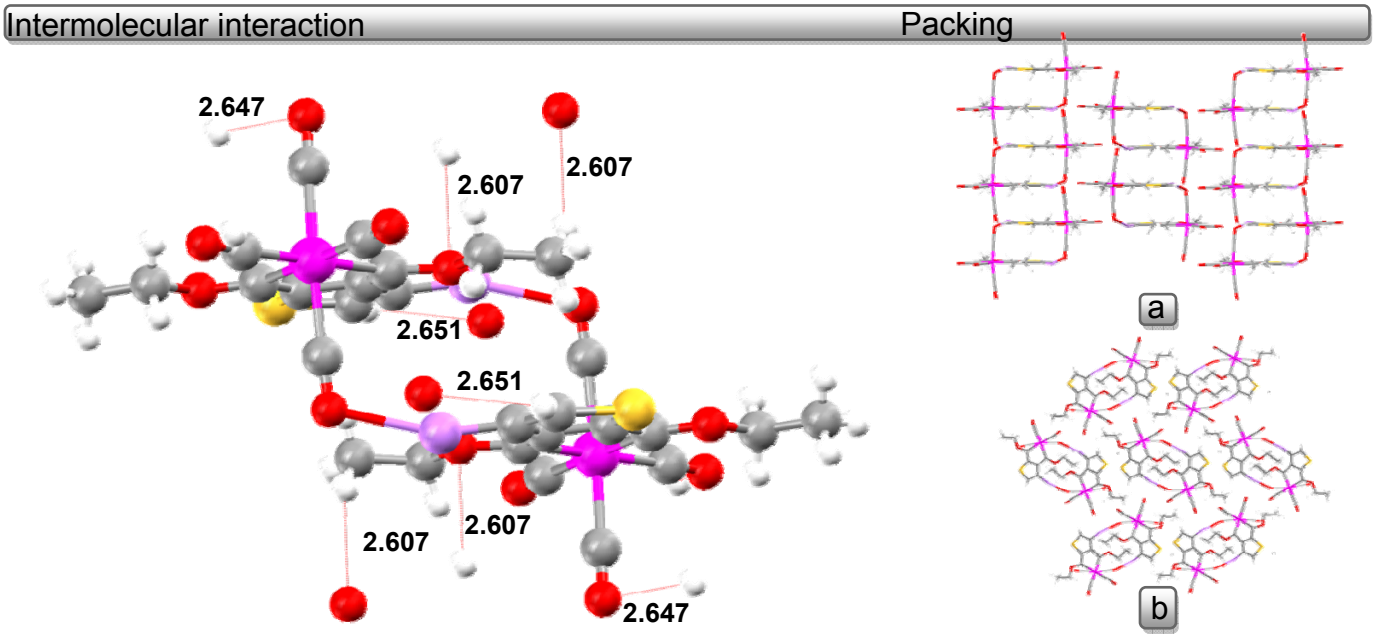

Figure 3.43: Intermolecular interaction and packing of B2a precursor.

Overall, there were eight hydrogen interactions to six neighbouring molecules. As with complex **B1** there were hydrogen interactions to either side of the complex but in this case the interactions were to four neighbouring molecules. There were additional hydrogen interactions to the molecule above and below the plane of the thienyl ring. Similar to complex **B3** the plane of the thienyl rings was not parallel. The packing was not as ordered as those discussed above but similar in the fact that the polar and non-polar groups orientate together (b). Interestingly, the thienyl groups are not orientated above one another. Instead the chelate formed, by the two carbene metal moieties were above the ethoxy groups.

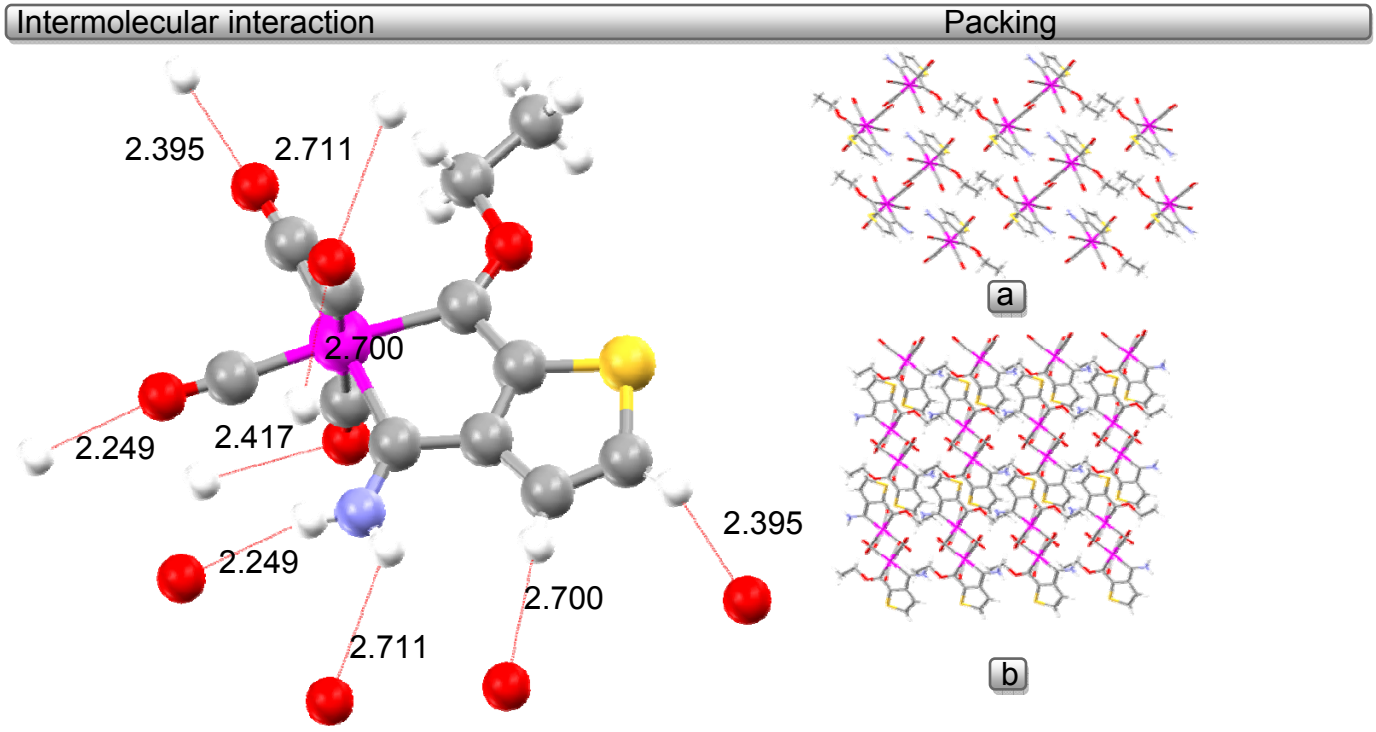

Figure 3.44: Intermolecular interaction and packing of B5.

The packing of compound **B5** also showed interaction to both sides resulting in a chain formation with all molecules in the same orientation (Figure 3.44). Each chain was bonded to each other in the chain in the same plane but in a reverse direction. There was interaction to one molecule above and two below the plane. The grid-like pattern observed for **B1** and **B3** was not evident from the packing pattern of **B5**. The packing showed that the metal ligands orientate themselves together in a very ordered fashion (Figure 3.44, b). The interaction of one molecule to nine other atoms resulted in the alternate orientation of neighbouring molecules, distancing the thienyl ring to be oriented in organic layers with the ethoxy groups.

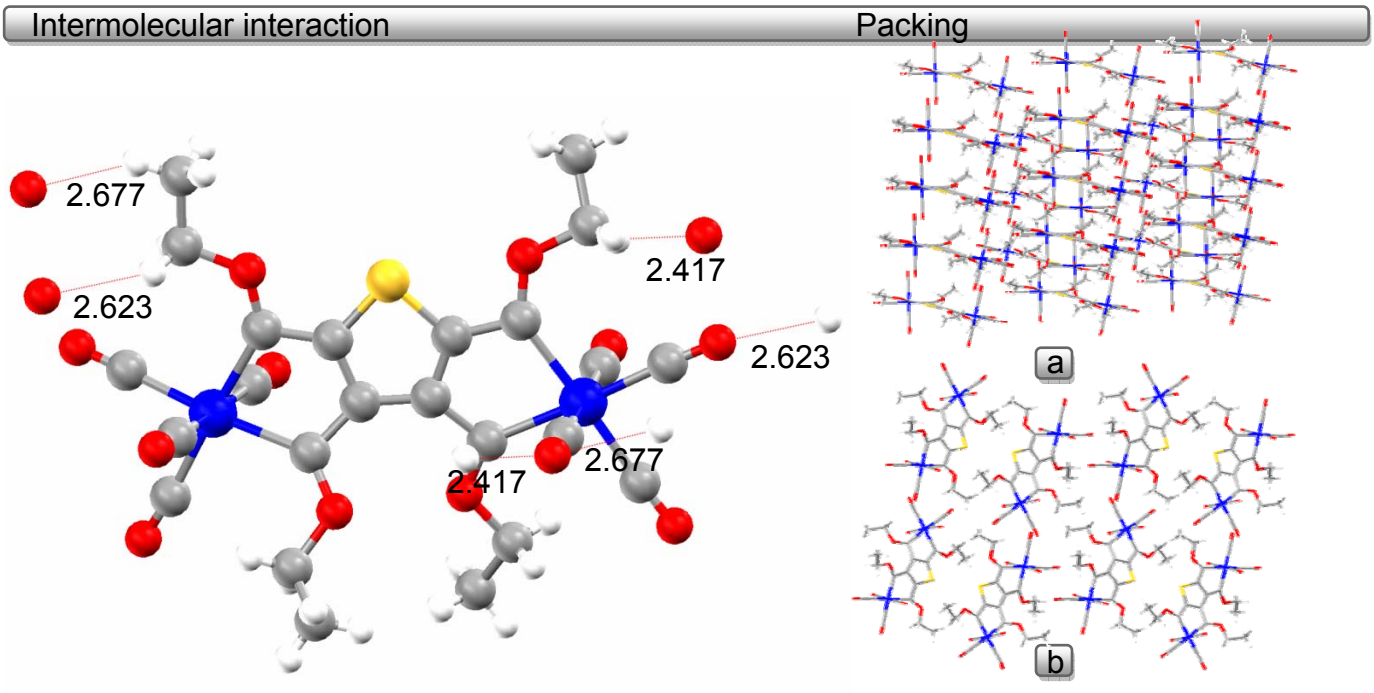

Figure 3.45: Intermolecular interaction and packing of B7.

Complex **B7** shows six interactions to seven other complexes (Figure 3.45). The rings were slightly bent inwards (a) and alternate packing causes a space inside the complex (c). The molecules were packed in a sliding pattern (b) with the same orientation to the flanking molecule. This results in sheets of molecules with alternating orientation.

Chapter 4: Experimental

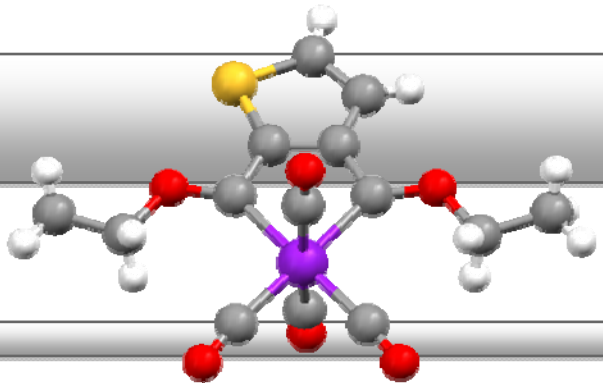

Syntheses and separations

Standard operational procedures

Syntheses were done using standard Schlenck techniques. All syntheses and characterizations were done under inert conditions using argon and nitrogen to create an inert atmosphere. Solvents were prepared by drying under inert conditions using standard laboratory techniques specified for each solvent. THF, ether, toluene and hexane were dried on sodium metal and DCM with P_2O_5. Butyllithium stock solution of 1.6 M in hexane was stored under argon in a dark bottle when required the desired quantity was transferred according to required operational procedures. Separation was done using chromatographic separation techniques with Kieselgel 60 (particle size: 0.0063-0.200 mm) and increasing the polarity of the solvent gradually or as otherwise specified. Chemicals were used as bought or unless stated differently. Crystallization was done by dissolving the complex in the minimum amount of polar solvent, DCM, ether or toluene by layering with the same amount of hexane. The solution was sealed under argon gas and allowed to crystallize over several days at 0ºC or -15ºC.

Characterization techniques

Nuclear magnetic resonance spectra

NMR spectra were recorded on Bruker AC-300, AC-400 and AC-500 nuclear magnetic resonance spectrometers. ^{1}H-NMR spectra were measured at 300.135, 400.21 and 500.13 MHz for the respective instruments and the ^{13}C-NMR spectra were measured at 75.47, 100.63 and 125.76 MHz. Deuterated reference solvents were specified for each measurement as $CDCl_3$ or C_6D_6. The ^{1}H and ^{13}C-NMR resonances for the reference peak of $CDCl_3$ was at 7.260 and 77.16 ppm respectively and for C_6D_6 at 7.160 and 128.060 ppm [1]. All samples were prepared under inert conditions and sealed under argon just before data collections.

Infrared spectroscopy

Infrared spectra were obtained on a Perkin-Elmar RXI FT- infrared spectrometer using a NaCl cell and dried hexane as solvent. Before measurements the machine was calibrated using the same dried hexane solvent.

Ultraviolet Spectroscopy

A dry quartz cell was used and hexane as solvent which was also used as reference solution. The measurements were done in a window of 200 – 700 nm.

[1] H.E. Gottliebe, V. Kotlyar, A. Nudelman, *J. Org. Chem.,* **1997***, 62*, 7512

X-Ray crystallography

A Bruker/Siemens P4 diffractometer was used to obtain crystallographic data with a Bruker Smart 1K CCD detector using a graphite monochromated, MoKα radiation at 20º angle with phi and omega scans unless stated otherwise. Data collection was done with Lorenz polarization effects and structure elucidation was done with SHELXS[2] and refined by full-matrix least square methods.

Mass spectrometry

A VG70Se instrument was used to obtain FAB spectra and a Thermo DFS for accurate mass measurements with nba as a matrix.

Computational Chemistry

Electron distribution data were obtained from Gaussian 04 package using Gaussview 3[3]. Structures were optimized using density functional theory with a B3LYP functional and a LANL2DZ basis set.

[2] SHELXTL version 6.12, Bruker AXS Inc. **2001**, Madison W1, USA, G.M. Sheldrick, SHELXL-97, University of Göttingen, Germany, **1997**

[3] M. J. Frisch, G. W. Trucks, H. B. Schlegel, P. M. W. Gill, B. G. Johnson, M. A. Robb, J. R. Cheeseman, T. A. Keith, G. A. Petersson, J. A. Montgomery, K. Raghavachari, M. A. Al-Laham, V. G. Zakrzewski, J. V. Ortiz, J. B. Foresman, J.Cioslowski, B. B. Stefanov, A. Nanayakkara, M. Challacombe, C. Y. Peng, P. Y. Ayala, W. Chen, M. W. Wong, J. L. Andres, E. S. Replogle, R. Gomperts, R. L. Martin, D. J. Fox, J. S. Binkley, D. J. Defrees, J. Baker, J. J. P. Stewart, M. Head-Gordon, C. Gonzalez, J. A. Pople, *Gaussian 94*, **1995,** Revision D1, Gaussian, Inc., Pittsburgh, PA,

Synthesis and purification of starting materials

Triethyloxonium tetrafluoroborate[4], triaminetricarbonyl chromium and chromium (η^5-thiophene) tricarbonyl[5] were prepared as described in literature. Chromium (η^5-3-bromothiophene) tricarbonyl was synthesized using the same method as chromium (η^5-thiophene) tricarbonyl [5] by replacing thiophene with 3-bromothiophene. Thiophene was purified according to literature[6] and stored under argon in a dark container.

Synthesis

Synthesis of dinuclear biscarbene complexes (A1-5)

Synthesis for complex **A1** is described below. The same reaction conditions were applied to the synthesis of all 5 complexes, **A1-5** and the reagent amounts used are listed in Table 4.1. Experimental observation such as colour changes differed only in intensity and deviations are as stated.

Method

At -90ºC, 0.44 g (2 mmol) of chromium (η5-thiophene) tricarbonyl was dissolved in THF, and was reacted with 1.35 ml (2 mmol) BuLi while vigorously stirring. The solution was allowed to warm slightly until the clear red-orange solution turned yellow. The solution was cooled and a

[4] H. Meerwein, *Org. Synth.,* **1966***, 46*, 113
[5] M. Novi, G. Guanti, C. Dell'Erba, *J. Heterocycl. Chem.,* **1975,** *12*, 1055
[6] G.H. Spies, R.J. Angelici, *Organometallics* ,**1987***, 6,* 1902

second equivalent of BuLi (2 mmol) was added at -90ºC. The temperature was allowed to rise until a colour change was observed. The metal carbonyl complex ($Cr(CO)_6$) 0.88 g (4 mmol) was added to the solution at -60ºC and a colour change to dark red was observed. The reaction mixture was allowed to rise to room temperature and the solvent was removed under vacuum. The reaction mixture was resuspended in DCM and cooled to -35ºC. A pre-prepared mixture of triethyloxonium tetrafluoroborate in DCM with a known concentration was slowly added to the solution, where by colour change from red to purple was observed, after which the solution was allowed to warm to room temperature. The stoichiometric amount of triethyloxonium tetrafluoroborate was 0.76 g (4 mmol) added but an additional excess of ± 30% was used as required. The alkylation process was followed with thin layer chromatography to determine the amount of excess triethyloxonium tetrafluoroborate needed.

Table 4.1: Summary of reagent quantities used for synthesis of A1-5.

Complex	Metal ligand	$(\eta^5\text{-}C_4H_4S)Cr(CO)_3$	BuLi	$[Et_3O][BF_4]$
Quantity				
A1	0.88 g (4 mmol) $Cr(CO)_6$	0.44 g (2 mmol)	2.9 ml (4 mmol)	0.76 g (4 mmol)
A2	1.1 g (4 mmol) $Mo(CO)_6$	0.44 g (2 mmol)	2.9 ml (4 mmol)	0.76 g (4 mmol)
A3	1.1 g (3.2 mmol) $W(CO)_6$	0.40 g (1.6 mmol)	2.8 ml (3.2 mmol)	0.60 g (3.2 mmol)
A4	0.41 g (2 mmol) $MnCp(CO)_3$	0.22 g (1 mmol)	1.0 ml (2 mmol)	0.38 g (2 mmol)
A5	0.65 g (1 mmol) $Re_2(CO)_{10}$	0.12 g (0.5 mmol)	0.63 ml (1 mmol)	0.19 g (1 mmol)

Separation

After alkylation the solvent was evaporated under reduced pressure and the reaction mixture was placed on a silica gel column. The respective bands were separated using gradient elution, starting with hexane and increasing the polarity with DCM. The three bands consisted of butyl carbene complex of chromium, unreacted starting material and the purple coordinated biscarbene product. Complex **A5** showed 6 purple products using TLC but only the major purple band could be separated using column chromatography. The product colour and yields are listed below (Table 4.2). Other minor products were not purified.

Table 4.2: Summary of the target products colour and yields in percentage.

Complex	Colour	Mass (g)	Yield (%)
A1	Purple	0.43	30
A2	Purple	0.33	20
A3	Purple	0.56	35
A4	Purple	0.070	10
A5	Purple	0.080	10

Table 4.3: Elemental analysis data of A1-5.

Elemental Analysis										
	Calc.	Found	Calc.	Found	Calc.	Found	Calc.	Found	Calc.	Found
Complex	**A1**		**A2**		**A3**		**A4**		**A5**	
C	30.46	30.21	35.23	34.94	28.46	28.23	48.15	47.80	24.09	23.89
H	1.93	1.91	1.72	1.71	1.43	1.42	3.46	3.49	0.88	0.87

Synthesis of dinuclear biscarbene complexes (A6)

Method

To 0.17 g (0.51 mmol) of QTP dissolved in THF, 1.1 ml (1.7 mmol) BuLi was added at -70ºC and allowed to react. The solution turned from clear yellow to turquoise. 0.22 g (1 mmol) of $Cr(CO)_6$ was added to the reaction mixture that was allowed to rise to room temperature and the solvent was removed under vacuum. The reaction mixture was resuspended in DCM and cooled to -35ºC. A pre-prepared mixture of triethyloxonium tetrafluoroborate in DCM with a known concentration was slowly added to the solution where by a colour change to purple was observed, after which the solution was allowed to warm to room temperature. The stoichiometric amount of triethyloxonium tetrafluoroborate was 0.19 g (1 mmol) but an additional excess of ± 30% was used as required. The alkylation process was followed with thin layer chromatography to determine the amount of excess triethyloxonium tetrafluoroborate needed. Four bands were observed, a yellow zone consisting of starting material, a pink band and the purple biscarbene complex, **A6**.

Separation

After alkylation the solvent was evaporated under reduced pressure and the reaction mixture was filtered using silica gel. Solvent was removed *in vacuo*. The reaction mixture was resuspended in DCM and adsorbed on silica gel. The adsorbed reaction mixture was placed on a column and separated using gradient elution. Starting with hexane and increasing the polarity with DCM. The bands observed consisted of unreacted starting material, the suspected monocarbene complex that quickly decomposed and **A6** with a 20% yield (0.084 g). Anal. Calc. for $[Cr(CO)_5\{C(COEt)2,5\text{-}C_{16}H_8S_4C(OEt)\}Cr(CO)_5]$: C, 46.49; H, 2.19. Found: C, 46.11; H, 2.17.

Synthesis of mononuclear biscarbene complex (B1)

Two methods were used to synthesize complex **B1** with different starting materials and are reported below.

Method

At -10ºC, 0.50 g (3 mmol) of 3-bromothiophene in THF was reacted with 2.14 ml (3 mmol) of BuLi. A 1:1 mixture of 0.41 ml (3 mmol) LDA and 2.14 ml (3 mmol) BuLi was prepared in THF and added to the mixture at -78ºC. The solution was allowed to react and warm to room temperature after which 0.66 g (3 mmol) $Cr(CO)_6$ was added. The solution was warmed to RT and the solvent was removed under vacuum. After resuspending the reaction mixture in DCM a pre-prepared mixture of triethyloxonium tetrafluoroborate in DCM with a known concentration was slowly added to the solution at -30ºC. The stoichiometric amount of triethyloxonium

tetrafluoroborate was 1.15 g (6 mmol) but an additional excess of ± 30% was used as required. The alkylation process was followed with thin layer chromatography to determine the amount of excess triethyloxonium tetrafluoroborate needed.

Separation

After alkylation, the solvent was evaporated under reduced pressure and the reaction mixture was filtered through silica gel. The solvent was removed and the reaction mixture adsorbed on silica gel from a DCM solution. The adsorbed mixture was placed on a silica column and the reaction products was separated with gradient elution using hexane and by increasing the polarity with DCM. The three bands consisted of butyl carbene complex of chromium, yellow (10%), a red monocarbene complex (50%) and a blue biscarbene monochelate complex (**B1**), 40% (0.43 g). Anal. Calc. for $[Cr(CO)_4\{C(OEt)2,5\text{-}C_{16}H_8S_4C(OEt)\}]$: C, 46.67; H, 3.36. Found: C, 46.29; H, 3.33.

Synthesis of mononuclear biscarbene complexes (B1-3 and B6-7)

The synthesis of complex **B1** is described below. The same reaction conditions were applied to the synthesis of all complexes **B1-3, B7-8** and reagent quantities were reported in Table 4.4. Complex **B1** and **B6** were collected as products from the same reaction as was complex **B3** and **B7**. Experimental observation as colour change differed only in intensity, deviations are as stated.

Method

At -95ºC, 0.39 g (1 mmol) of 2,3,4,5-tetrabromothiophene was dissolved in THF and reacted with 3 ml (2 mmol) BuLi with vigorous stirring. The solution was allowed to warm slightly until the clear solution turned yellow. The metal carbonyl complex 0.44 g (2 mmol) was added to the solution at -78ºC and a colour change from yellow to pink to purple was observed. The solution was cooled to -95 ºC and a second equivalent, 3 ml (2 mmol) of BuLi, was added. The temperature was allowed to rise to room temperature and the solvent was removed under reduced pressure. The reaction mixture was resuspended in DCM and cooled to -35ºC. A pre-prepared mixture of triethyloxonium tetrafluoroborate in DCM with a known concentration was slowly added to the solution where by a colour change from purple to black was observed, after which the solution was allowed to warm to room temperature. The stoichiometric amount of triethyloxonium tetrafluoroborate was 0.76 g (4 mmol) but an additional excess of ± 50% was used as required. The alkylation process was followed with thin layer chromatography to determine the amount of excess triethyloxonium tetrafluoroborate needed.

Reagent quantities

Table 4.4: Summary of reagent quantities used for synthesis of B1-3 and B6-7.

Complex	Metal ligand	C_4Br_4S	BuLi	$[Et_3O][BF_4]$
	Quantity			
B1,6	0.44 g (2 mmol) $Cr(CO)_6$	0.39 g (1 mmol)	2.5 ml (4 mmol)	0.76 g (4 mmol)
B2,7	0.52 g (2 mmol) $Mo(CO)_6$	0.39 g (1 mmol)	2.5 ml (4 mmol)	0.76 g (4 mmol)
B3	0.70 g (2 mmol)	0.39 g (1 mmol)	2.5 ml (4 mmol)	0.76 g (4 mmol)

Separation

After alkylation the solvent was evaporated under reduced pressure and the reaction mixture was placed on a silica gel column. The respective bands were separated using gradient elution starting with hexane and increasing the polarity with DCM. Several bands were observed with three main products. A red band consisted of isomers of the monocarbene complex, a blue band composed of the biscarbene monochelate complex (**B1**) and a purple (**B6**) bischelate tetracarbene complex. The product colour and yields are listed below (Table 4.5).

Table 4.5: Summary of the reaction products colour and yield using tetrabromothiophene as starting material.

Complex	Colour	Mass (g)	Yield (%)
B1	Blue	0.11	30
B6	Purple	0.13	20
B2	Purple	0.10	25
B3	Blue	0.098	20
B7	Black	0.079	15

Table 4.6: Elemental analysis data of B1-3 and B6, 7.

Elemental Analysis										
	Calc.	Found	Calc.	Found	Calc.	Found	Calc.	Found	Calc.	Found
Complex	**B1**		**B2**		**B3**		**B6**		**B7**	
C	46.67	46.29	41.60	41.26	34.17	33.89	45.29	44.92	32.02	31.76
H	3.36	3.33	2.99	2.97	2.46	2.44	3.17	3.14	2.24	2.22

Synthesis of mononuclear biscarbene complex (B4)

Method

At -95ºC, 0.29 g (1 mmol) of chromium (η^5-3-bromothiophene) tricarbonyl, THF was reacted with 1.3 ml (2 mmol) of BuLi. A change was observed from red to light orange and an orange precipitate formed. The solution was allowed to react after which 0.22 g (1 mmol) $Cr(CO)_6$ was added at -95ºC. The solution was warmed to RT and the solvent was removed under vacuum. After resuspending the reaction mixture in DCM, a pre-prepared mixture of triethyloxonium tetrafluoroborate in DCM with a known concentration was slowly added to the solution. The stoichiometric amount of triethyloxonium tetrafluoroborate, 0.19 g (1 mmol), was added but an additional excess of ± 50% was required. The alkylation process was followed with thin layer chromatography to determine the amount of excess triethyloxonium tetrafluoroborate needed.

Separation

After alkylation the solvent was evaporated under reduced pressure and the reaction mixture was placed on silica gel. Using TLC multiple products were observed but not identified due to their low yield but two major zones were collected. The two bands were observed as a bright orange to red band that was determined to be monocarbene complexes (80%) and a dark purple band, **B4** that afforded 0.10 g. The bands were separated using gradient elution with hexane and increased polarity using DCM. Anal. Calc. for [(Cr{2,3-C(OEt)η^5-C_4H_2SC(OEt)}$(CO)_4$)Cr$(CO)_3$]: C, 42.3; H, 2.96. Found: C, 41.9; H, 2.94.

Synthesis of mononuclear biscarbene complex (B5)

Method

Pure crystalline **B1**, 0.11 g (0.29 mmol) was suspended in ether and ammonia gas bubbled through the solution for approximately 10 minutes. The degree of aminolysis was followed with TLC and continued until only a small amount of the original starting material was left. Two products were observed. The first was the original complex **B1** and the second complex **B5** (0.091 g, 90%). Additional ammonia resulted in the formation of multiple blue products, which quickly decomposed to brown products.

Separation

The ether solution was concentrated by evaporation and an equivalent amount of hexane was added. The complex was allowed to crystallize out of the solution over time at 0ºC. Anal. Calc. for [Cr{2,3-C(OEt)C_4H_2SC(NH_2)}$(CO)_4$]: C, 43.5; H, 2.74. Found: C, 43.2; H, 2.72.

Chapter 5: Summary

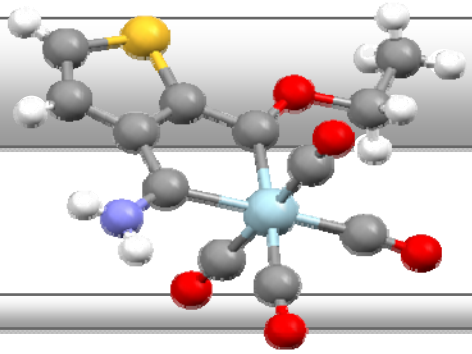

Monolithiation of thiophene was readily achieved at -30ºC in THF by *n*-butyl lithium. By contrast, to effectively dilithiate required much harsher reaction conditions. Typically dilithation was achieved at 60ºC in hexane with TMEDA activated BuLi. The activation of a thienyl moiety towards dilithiation was possible by addition of extra thiophene units on the 2,5 position of thiophene. The synthesis of the biscarbene complex **A1** $[Cr(CO)_5\{C(OEt)2,5\text{-}C_{16}H_8S_4C(OEt)\}Cr(CO)_5]$ on quaterthiophene was accomplished at low temperatures with satisfactory yields but the monocarbene complex could not be isolated. The biscarbene complex was relatively stable for prolonged periods of time and show similar characteristics as colour, chemical shift pattern and carbonyl stretch patterns, to reported biscarbene complexes on thienyl derivatives[1]. From calculated data, communication between the metal fragments due to the conjugated system was not possible as the electron density was localized to the double bond regions. This was supported by the structural data showing the metal carbonyl fragments were out of plane resulting in molecules packing in a slide.

The $Cr(\eta^5\text{-}C_4H_4S)(CO)_3$ thiophene analogue was readily lithiated at 2 and 5 position due to the increased acidity of the protons on these positions resulting from the electron draining character of the chromium tricarbonyl fragment. Yields obtained from the synthesis of the biscarbene complexes **A1-5** varied but the relative stability of these complexes above -15ºC were very low. The insertion of THF was not observed, as with the reported monocarbene

[1] (a) Y.M. Terblans, PhD Thesis, *Thiophene bimetallic carbene complexes*, **1996**, University of Pretoria
(b) M.M. Moeng, MSc dissertation, *Terthienyl carbene complexes,* **2001**, University of Pretoria

analogue[2] and consideration of the difference of reaction conditions might be the reason. Monolithiation was reported at -40ºC, whereas reaction conditions used here were carried out at -90ºC. From NMR spectroscopic studies it was detected that there is restricted rotation around the carbene bonds resulting in signal duplication due to different chemical environments. Chemical shift values for all complex **A1-5** were shifted upfield due to the presence of the tricarbonyl fragment and the range were in good agreement with those reported for the similar monocarbene complexes of chromium and tungsten[2]. The duplication of almost all chemical shift values in different ratios for the ^{13}C-NMR spectrum of complex **A1** suggested preferred geometrical isomers. IR studies showed the presence of both pentacarbonyl and tricarbonyl stretches and these bands overlap. Only small quantities were available for the reaction syntheses due to the amount of starting material that could be synthesized at one time. Synthesis of a larger amount of the $Cr(\eta^5\text{-}C_4H_4S)(CO)_3$ in a particular reaction was not possible due to the size and the availability of the pressure flask. Complete characterization of these complexes immediately after separation is advisable.

Another way of activating the 2,5-positions for lithiation was achieved by using 2,5-dibromothiophene as precursor. Dilithiation was obtained at -30ºC in THF with 4 equivalents of BuLi. This raised the question whether it would be possible, synthetically, to activate all four positions of thiophene and prepared a 2,3,4,5-tetracarbene thiophene. This would be the first time that all available positions of a heteroarene will be lithiated and transformed into Fischer carbene ligands. To achieve this a number of synthetic challenges had to be overcome. The greatest challenge was to activate the 3 and 4 positions of thiophene and initial work with 3-bromothiophene showed how this goal could be achieved. At very low temperatures (-90ºC) the 3-position could be lithiated and the kinetic product stabilized. At this stage a metal carbonyl was added. In addition 3-bromothiophene was coordinated to chromium tricarbonyl to form the precursor, chromium η^5-(3-bromothiophene) tricarbonyl. Addition of lithium at -90ºC to 3-bromothiophene or chromium η^5-(3-bromothiophene) tricarbonyl resulted in the formation of the corresponding lithium derivative at position 3, which afforded the metal acylate when the chromium hexacarbonyl was added. In a second step, llithiated at the 2 position to afford a metal bisacylate and after subsequent alkylation produced **B4**. The neutral carbene

[2] Y.M. Terblans, S. Lotz, *J. Chem. Soc., Dalton Trans.*, **1997**, 2177

chelate complexes **B1-3** was synthesized in this manner. The synthesis of $Cr(\eta^5$-3-$C_4H_3BrS)(CO)_3$ allowed for the formation of **B4** $[Cr\{C(OEt)\eta^5$-2,3-$C_4H_2SC(OEt)\}(CO)_4)Cr(CO)_3]$ following the same synthetic procedure as with 3-bromothiophene. The complexes **B1** $[Cr\{C(OEt)2,3\text{-}C_4H_2SC(OEt)\}(CO)_4]$ and **B4** $[Cr\{C(OEt)\eta^5\text{-}2,3\text{-}C_4H_2SC(OEt)\}(CO)_4)Cr(CO)_3]$ were obtained in a reasonable yield.

It was possible to activate the 3 and 4 position of thiophene along with the 2 and 5 position by the use of 2,3,4,5-tetrabromothiophene. The activation energy pattern of these positions were similar to those of free thiophene with the 2 and 5 position being the most activated, but contrary to free thiophene the 3 and 4 position was also lithiated by lithium-halogen exchange using the same conditions as for the 2 and 5 position. Lithiation at the 2 and 5 positions followed by addition of the metal hexacarbonyl and subsequent lithiation of the 3 and 4 positions followed by alkylation afforded the carbene bischelate complex **B6** $[2,3,4,5\text{-}C_4S\{C(OEt)\}_4\{Cr(CO)_4\}_2]$ and **B7** $[2,3,4,5\text{-}C_4S\{C(OEt)\}_4\{W(CO)_4\}_2]$. The synthesis of $[2,3,4,5\text{-}C_4S\{C(OEt)\}_4\{Mo(CO)_4\}_2]$ resulted in a complex of low stability which quickly decomposes to the ester analogue. Complex **B2** $[Mo\{C(OEt)2,3\text{-}C_4H_2SC(OEt)\}(CO)_4]$ and **B3** $[W\{C(OEt)2,3\text{-}C_4H_2SC(OEt)\}(CO)_4]$ was also obtained from these reactions.

The reactivity of these types of carbene monochelate complexes were tested by aminolysis by bubbling $NH_{3(g)}$ through a solution of **B1** in dissolved in ether. The monosubstitution of an ethoxy group from a biscarbene precursor complex was extraordinary and not previously reported in literature. Replacement of both ethoxy groups resulted in lengthening of the $C_{carbene}$-M bond and consequent opening of the chelate ring to form corresponding decomposition products. The substitution of only one ethoxy group supports the statement that there was selective stabilization to the carbene neighbouring the sulphur atom. The synthesis of two classic Fischer carbene chelates on a single arene or heteroarene has not yet been reported in literature. The properties of thiophene decorated Fischer carbene complexes or chelate carbenes needs further investigation and holds great promise for new and unique reaction pathways.

From spectroscopic data of complex **B1**, **B2** and **B3** it was observed that the thienyl ring protons on the 5 position were deshielded and shifted downfield compared to the monocarbene complex on the 2 position of thiophene[3]. The carbene ligands polarize the thienyl ring in an unsymmetrical manner resulting in the ring conjugation to only stabilize the carbene substituent in the two positions. The unequal stabilization results in chemical shifts of the ethoxy protons in the ^{1}H-NMR spectra to be apart with the more shielded ethoxy group shifted more downfield. The differences in ^{13}C-NMR chemical shift values for carbene carbons were also observed. Similarly, the ethoxy proton resonances of complexes **B6** and **B7** were separate but the molecules were symmetrical and the separation of chemical shift values for the ethoxy groups were only due to the presence of the sulphur atom on the one side of the molecule. The chemical shift of the ring protons of complex **B1** compared to that of **B4** was downfield. These upfield shifts of the arene proton resonances of complex **B4** were similar to that seen for complexes **A1-5**. The electron draining chromium tricarbonyl fragment withdraws electron density from the ring deshielding these protons. Similarly, the ethoxy proton resonances were duplicated due to the chemically differing environments of the two individual carbene ligands. The difference in backdonation from the respective heteroatoms on both the carbene monochelate and bischelate complex was not as pronounced in the crystal structure as in a dynamic system. The individual carbene chemical shifts were also seen in some cases as well as duplication of the ethoxy carbons resonances. From infrared spectra there were four characteristic carbonyl stretches for each carbonyl and UV spectra that showed four electron transitions. The carbene monochelate complexes pack as rigid grid-like structures and the packing of the carbene bischelate complex **B7** was more disordered. From the X-Ray diffraction data obtained it was observed that not all lithiums were hydrolyzed and lithium of one molecule interacted with the next carbene monochelate complex to form a square complex. These complexes were observed when using 2,3,4,5-tetrabromothiophene as a starting material and not 3-bromothiophene and were isomorphous to the carbene monochelate complexes obtained from the reaction using 2,3,4,5-tetrabromothiophene. Further investigation using computational techniques can lead to the determination of the π-conjugation of the system and the exact transfer of electrons from the specific orbitals.

[3] S. Gronowitz, *Adv. Heterocycl. Chem.*, **1963**, *1*, 1

The coordination of a metal ligand to activate a thienyl moiety was transferred from other compounds such as benzene to arene derivates. Such complexes were well established in literature[4] and allowed for further exploitation of activated areas to synthesize spacer type ligand consisting of multimetal systems. Elongation of the thienyl spacer allowing lithiation under mild conditions may only be transferable to other heteroarenes. This allows for diverse lengths if incorporated into a metal organic framework that may be used for selective catalysis. The application of halogen-lithium exchange to utilize selected positions on an organic moiety, with the aim to synthesize Fischer carbene complexes, show great promise. This method may allow for the amalgamation of multiple sites on one organic molecule to synthesize larger more complex carbene clusters working towards creation of a metal-organic-frameworks. The addition of a carbene functionalities to unactivated sites of thiophene and the formation of carbene chelates also permit for synthetic catalytic application to obtain organic substrate from these unactivated positions and cyclization of the carbene chelate. The difference in reactivity of one carbene ligand towards aminolysis is unique and could allow for catalytic organic synthesis, which has not previously been accessible. Application of this method to organic compounds such as benzene may allow for decoration of all six positions with carbene chelates. Hexalithiobenzene[5] is known but sequential lithiation and metal acylate formation may be the key to synthesize such complexes. As alternative methodology reports polymerization of benzene in the attempt to synthesize *o*-dilithiobenzene via lithium-halogen exchange[6].

In conclusion, thiophene could be activated *via* different methodologies, be it on the activated sites or non-activated sites. This allows for the synthesis of classic Fischer mononuclear and dinuclear biscarbene complexes and ultimately the synthesis of tetracarbene complexes on a

[4] (a) T.B. Rauchfuss, *Coord. Chem. Rev.,* **1991,** *39,* 259
(b) H. Braunschweig, F.M. Breitling, *Coord. Chem. Rev.,* **2006**, *250*, 2691
(c) D.A. Delafuente, W.H. Myers, M. Sabat, W.D. Harman, *Organometallics,* **2005**, *24*, 1876
(d) D.L. Kershner, F. Basolo, *Coord. Chem. Rev*.,**1987**, *19*, 279
(e) J. Chen, V.G. Young, Jr., and R.J. Angelici, *Organometallics* **1996,** *15*, 325
(f) M. Landman, T. Waldbach, H Görls, S. Lotz, J. *Organomet. Chem.,* **2003**, *678*, 5
(g) Y. Ding, M. He, Y. Niu, D. Wang, Y. Cui, S. Feng, J. Phys. Chem. A, **2009**, *113,* 10291
[5] L.G. Snedon, R.J. Lagow, *J.C.S. Chem. Comm.*, **1987**, 302
[6] G. Wittig, F. Bickelhaupt, *Angew. Chem.,* **1975**¸*69*, 93

single arene. The formation of the chelate carbenes allows for selective reactivity towards the resonance stabilized carbene ligand.

Chapter 6: Appendices

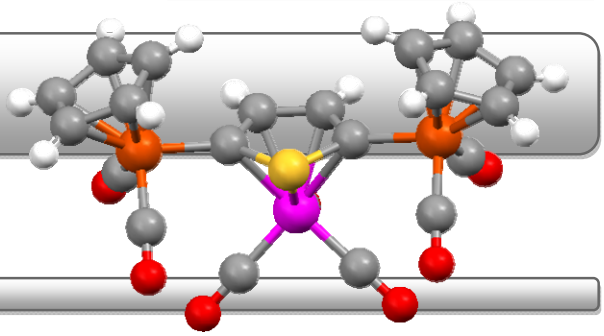

Supporting information

X-Ray diffraction data

Contains all CIF files obtained from X-Ray diffraction techniques for the complexes **A6**, **B1**, **B3**, **B2a**, **B3a**, **B5**, **B7**